



MEASUREMENT OF MULTIJET CROSS-SECTION RATIOS IN PROTON-PROTON COLLISIONS WITH THE CMS DETECTOR AT THE LHC

Anterpreet Kaur

Supervisor : Prof. Manjot Kaur

Department of Physics
Panjab University
Chandigarh, India

Outline

- Physics of the Thesis
- Experimental Set-up
- Theoretical Background
- Software Tools
- Analysis Strategy
- Measurement of Inclusive Multijet Cross-sections
- Theoretical Predictions
- Data-Theory Comparisons
- Cross-section Ratio R_{32}
- Determination of the Strong Coupling Constant, $\alpha_S(M_Z)$
- Summary and Outlook
- Hardware Activities

Physics of the Thesis

- The measurement of inclusive multijet event cross-sections,

$$\sigma_{i\text{-jet}} = \sigma(pp \rightarrow i \text{ jets} + X) \propto \alpha_S^i$$

*to be fixed in text

- ▶ and their ratio

$$R_{mn} = \frac{\sigma_m}{\sigma_n} \propto \alpha_S^{m-n}; m > n$$

- ▶ as a function of

$$\langle p_{T,1,2} \rangle = \frac{p_{T,1} + p_{T,2}}{2} = H_{T,2}/2$$

- The inclusive differential multijet event cross section is defined as :

$$\frac{d\sigma}{d(H_{T,2}/2)} = \frac{1}{\epsilon \mathcal{L}_{\text{int,eff}}} \frac{N_{\text{event}}}{\Delta(H_{T,2}/2)}, \text{ where}$$

- ϵ : the product of the trigger and jet selection efficiencies and $> 99\%$,
- $\mathcal{L}_{\text{int,eff}}$: the effective integrated luminosity,
- N_{event} : the number of 2- or 3-jet events counted in an $H_{T,2}/2$ bin, and
- $\Delta(H_{T,2}/2)$: the bin widths. The measurements are reported in units of (pb/GeV).

- In the talk :

- ▶ Highlighted text in green → changed during ARC review
- ▶ Inclusive 2-jet : $n_j \geq 2$ (300–2000 GeV), Inclusive 3-jet : $n_j \geq 3$ (300–1680 GeV),
Inclusive 4-jet : $n_j \geq 4$ (only in AN for now) and ratio : R_{32} (300–1680 GeV)

Introduction

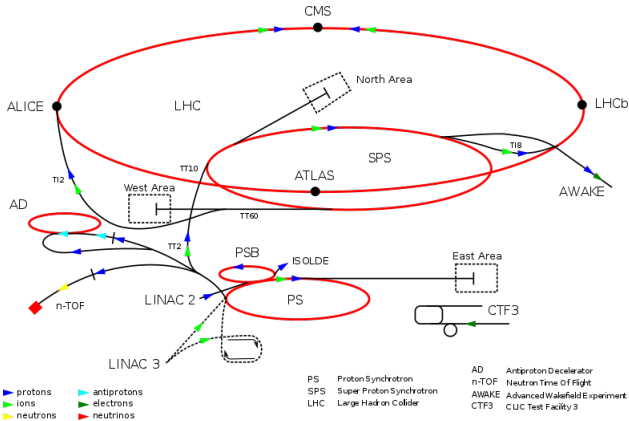
- Jets are the observable objects to relate experimental observations to theory predictions formulated in terms of partons.
- The events containing multiple jets in the final state are plentiful and provide a fertile testing ground for Quantum Chromodynamics (QCD).
- Inclusive jet cross-section is important to study as it provides precise measurement of α_S .
- **Why cross-section ratios ?**
 - better choice w.r.t. inclusive cross-sections because of less dependency on uncertainties such as :
 - uncertainties due to luminosity,
 - scale dependence,
 - PDF dependence etc.
- Definition of Cross sections ratios : $R_{n+1,n} = \frac{\sigma_{(n+1)\text{jet}}}{\sigma_{(n)\text{jet}}}$
- The ratios R_{32} , R_{43} , $R_{54} \approx \alpha_S$ and R_{42} , $R_{53} \approx \alpha_S$.
- A measurement of the ratio of the inclusive 3-jet cross section to the inclusive 2-jet cross section as a function of the average transverse momentum, $\langle p_{T1,2} \rangle$, of the two leading jets in the event is performed at 7 TeV ([Eur. Phys. J. C 73 \(2013\) 2604](#))



Images/jet2.png

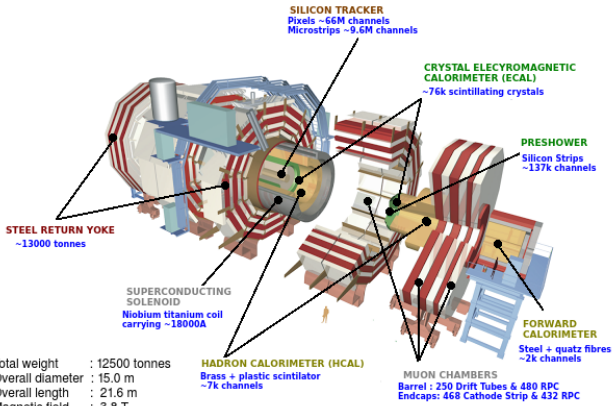
Large Hadron Collider

- World's biggest and the most powerful particle accelerator and collider built by CERN (European Organization for Nuclear Research)
- Located in a 27 km long tunnel, 100 m (approx.) underground at Swiss-France border.
- Proton-proton (p-p),** proton-lead and lead-lead as well as xenon-xenon nuclei collisions take place at different center-of-mass energies (\sqrt{s}).
- Currently running at $\sqrt{s} = 13 \text{ TeV}$ with peak luminosity, $\mathcal{L} = 2.1 \times 10^{34} \text{ cm}^{-2}\text{sec}^{-1}$.
- Four big experiments located at different interaction points.



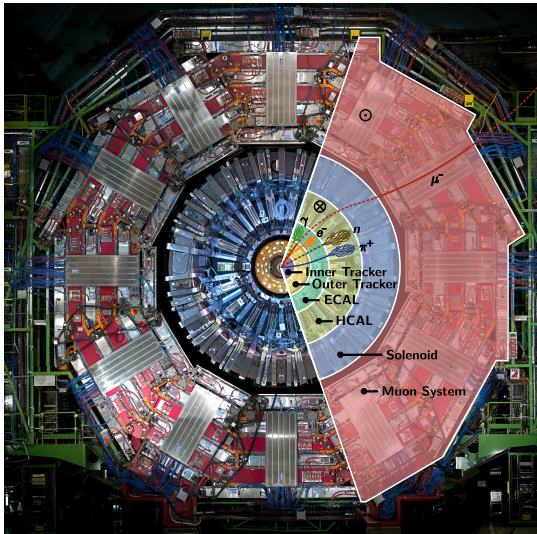
CMS Detector

- Compact Muon Solenoid (CMS) : One of the general purpose detectors which
 - is **compact** in size : 21 m long, 15 m wide and 15 m high weighing 12,500 tonnes
 - emphasis on the detection of **muons**
 - is enclosed within high **solenoidal** magnetic field
- Complex layered structure of sub-detectors : Tracker, Electromagnetic Calorimeter (ECAL), Hadron Calorimeter (HCAL) and Muon System.



CMS Detector : Front View

- Major fraction of the particles produced in p-p collisions is hadrons.
- Collimated in the form of conical structures called **Jets**.
- Both hadronic (charged and neutral) and electromagnetic components.
- Charged Particles** : energy deposits in the calorimeters.
- Neutral Particles** : missing transverse energy.
- HCAL** : detects neutral particles; an essential sub-system of the CMS detector and contributes to most of physics studies with CMS.



○ - Direction of magnetic field in the return yoke
⊗ - Direction of magnetic field inside the solenoid

Standard Model

- A theoretical model to describe the nature and properties of fundamental particles and their interactions.
- Fundamental particles :

▶ Fermions

- Quarks (q)
- Leptons (ℓ)

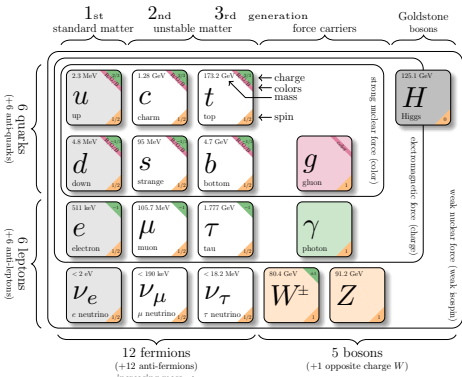
▶ Bosons

- Gauge Bosons
- Scalar Boson

- Forces of interactions :

- ▶ Electromagnetic - photon (γ)
- ▶ Strong - gluons (g)
- ▶ Weak - W^\pm and Z
- ▶ Gravity[★] - graviton

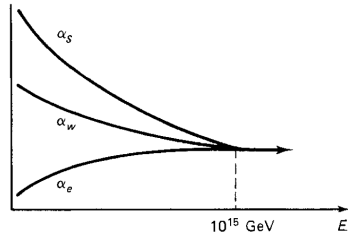
- Described by $\underbrace{SU(3)_C}_{\text{Strong}} \otimes \underbrace{SU(2)_L \otimes U(1)_Y}_{\text{ElectroWeak}}$ gauge symmetry



Quantum Chromodynamics (QCD)

- A non-abelian gauge theory describing the strong interactions between quarks and gluons.
- Color charge -
 - ▶ Quarks and gluons : colored
 - ▶ Hadrons - Baryons (qqq) and Mesons ($q\bar{q}$) : colorless
- Strong coupling constant α_S - a fundamental parameter giving the strength of interaction.
- Properties -
 - ▶ Confinement : at low energies → Non-perturbative (NP) regime
 - ▶ Asymptotic freedom : at high energies → Perturbative regime
- In perturbative QCD

$$X = \sum_{i=0}^N \alpha_s^n c_i = c_0 + \alpha_s^1 c_1 + \alpha_s^2 c_2 + \dots$$

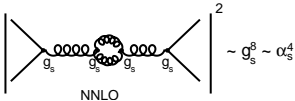
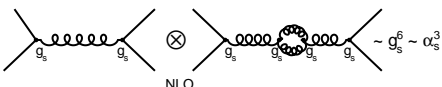
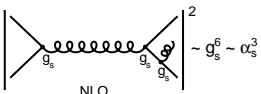
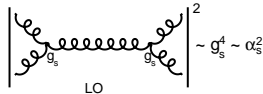
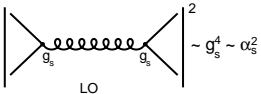


is determined by summing over the amplitudes of all Feynman diagrams.

- ▶ Power of α_S : the number of vertices associated with $q-g$ or $g-g$ interactions.

Perturbative QCD

Different orders in a $2 \rightarrow 2$ scattering process



$$\alpha_S(Q) = g_s^2 / 4\pi$$

- **Ultraviolet (UV) divergences :** Calculations become complex with the loop diagrams; associated integrals are divergent.
- **Renormalization :** a mathematical procedure which
 - ▶ allows finite calculation of momenta integrals of virtual loop by removing UV divergences.
 - ▶ introduces a regulator for the infinities - **renormalization scale μ_r** .
 - ▶ redefines or renormalizes the coupling constant to absorb the UV divergences.

Running of the Strong Coupling

- Renormalization group equation (RGE) : exact dependence of $\alpha_s(\mu_r^2)$ on μ_r

- ▶ Dependence of X on μ_r must cancel →

$$\mu_r^2 \frac{d}{d\mu_r^2} X \left(\frac{\mu^2}{\mu_r^2}, \alpha_s(\mu_r^2) \right) = 0$$

- ▶ First order solution of RGE is :

$$\alpha_s(\mu_r^2) = \frac{1}{b_0 \ln(\mu_r^2/\Lambda_{QCD}^2)}$$

- ▶ Coupling becomes large at the scale Λ_{QCD}
- ▶ For $b_0 > 0$, coupling becomes weaker at higher scales $Q \rightarrow$ asymptotic freedom

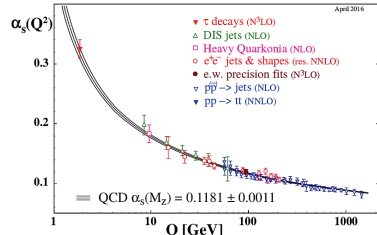
- It is always convenient to express α_s at some fixed scale -

- ▶ Some of the best measurements come from Z decays : the strong coupling is determined at the scale of the Z boson mass $\alpha_s(M_Z)$ given by

$$\alpha_s(\mu_r, \alpha_s(M_Z)) = \frac{\alpha_s(M_Z)}{1 + \alpha_s(M_Z)b_0 \ln(\mu_r^2/M_Z^2)}$$

- α_s : a free parameter of QCD theory

- ▶ must be extracted from experimental measurements
- ▶ evolved to the scale of the Z boson
- ▶ current world average value* is $\alpha_s(M_Z) = 0.1181 \pm 0.0011$

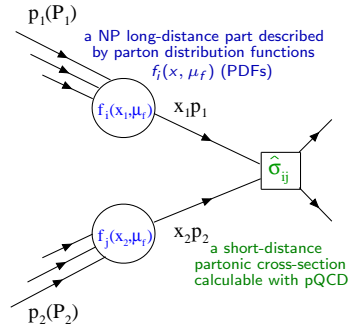


* Particle Data Group (PDG)

Hadronic Collisions

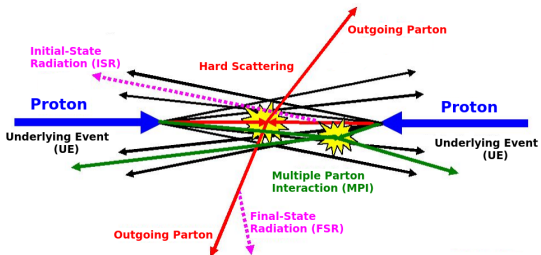
- **Proton** - three valence quarks (*uud*), gluons and the sea quarks.
- **Cross-section (σ)** of a certain process : the probability that the two hadrons interact and give rise to that final state.
- In a hadronic collision, the perturbation theory is only valid at the parton-level.
- **Factorization theorem** - allows the calculation of σ by separating into two parts :

$$\sigma_{P_1 P_2 \rightarrow X} = \sum_{i,j} \int dx_1 dx_2 f_{i,P_1}(x_1, \mu_f) f_{j,P_2}(x_2, \mu_f) \times \hat{\sigma}_{ij \rightarrow X} \left(x_1 p_1, x_2 p_2, \alpha(\mu_r^2), \frac{Q^2}{\mu_f^2} \right)$$



- ▶ Proton PDFs f_i and f_j : probability to find a parton i with momentum fraction x within a hadron.
- ▶ Factorization scale, μ_f : corresponds to the resolution with which the hadron is being probed.
 - Particles emitted with $p_T > \mu_f$ are considered in the calculation of hard scattering perturbative coefficients.
 - Particles emitted with $p_T < \mu_f$ are accounted for within the PDFs.

Hadronic Collisions



● Hard Scattering :

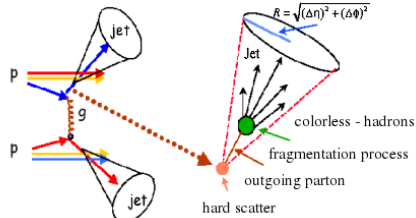
- ▶ Parton Shower : collinear parton splitting and the soft gluon emissions (pQCD).
- ▶ Hadronization : confinement of colored quarks and gluons into the color-neutral composite particles called hadrons (non-pQCD).

● Underlying Event : Event structure is significantly more complex than that of the lepton collisions.

- ▶ **Initial and Final-State Radiations (ISR, FSR)** : two incoming as well as outgoing partons can also develop parton showers.
- ▶ **Multiple Parton Interactions (MPI)** : remaining two partons which do not participate in a hard collision may also interact.

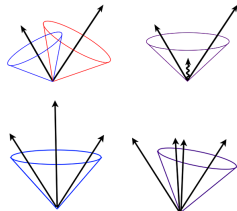
Jets

- Hadrons produced in p-p collisions get collimated in the form of conical structures called "jets" of radius ' R '.
- Direction of the jet is towards the direction of the initial partons that originated them.
- Detectable objects which relate experimental observations to theory predictions formulated in terms of partons.
- Act as a bridge between the elementary quarks and gluons of QCD and the final hadrons produced in high energy collisions.
- At the LHC, **Dijet Events** : $2 \rightarrow 2$, **Multijet Events** : $2 \rightarrow 3, 2 \rightarrow 4$
- Jets and their observables are the best tools to test the predictions of pQCD :
 - Jet production cross-section** : helps to extract the value of α_S and to reduce the uncertainties of the PDFs of the proton.
 - Inclusive multijet event cross-sections permits more elaborate tests of QCD.
 - A precise study of jet variables helps to understand the signal and background modelling for new physics searches in hadronic final states.



Jet Algorithms

- Jet algorithms provide a set of rules which determine how the particles can be clustered into a jet.
- Parameters involved indicate how close two particles must be to belong to the same jet :
 - ▶ Cone algorithms → closeness in coordinate space
 - ▶ Sequential Recombination algorithms → closeness in momentum space
- Recombination Scheme
- Infrared safety : Addition of a soft emission should not change the number of hard jets found in an event.
- Collinear safety : Collinear splitting should not modify the number of jets formed in an event.
- Three types of Sequential Recombination algorithms :
 - ▶ k_t : involves clustering of soft particles first; susceptible to the underlying and pileup events
 - ▶ Cambridge/Aachen (C/A) : involves energy independent clusterings.
 - ▶ anti- k_T : cluster hard particles first; less sensitive to underlying and pileup events.



Software Tools

- **CMS software (CMSSW) framework** : a dedicated data structure and software tools.
 - ▶ Performs calibration, event generation, detector simulation, event reconstruction etc. by implementing the codes either in C++ or Python languages.
- **ROOT** : an open source object-oriented data analysis framework.
 - ▶ Consists of a huge C++ library which store and analyze large amounts of the data.
 - ▶ Provides histogramming methods in 1, 2 and 3 dimensions, curve fitting functions, minimization procedures, graphics and visualization classes.
- **FASTJET** : a software C++ package.
 - ▶ Provides a broad range of jet finding, determination of jet areas, estimation of pileup and underlying-event noise levels etc.
- **NLOJET++** : a C++ program to evaluate jet production cross-sections at leading order (LO) and next-to-leading order (NLO).
 - ▶ Calculations of pQCD cross-sections using Monte Carlo integration methods are very time consuming.
 - ▶ PDF fits or estimations of uncertainties becomes difficult where the calculations of the cross-sections are needed to be repeated.
- **FASTNLO** : fast re-evaluations of cross-sections in interface with NLOJET++.
 - ▶ The strong coupling constant and the PDFs can be changed without a re-calculation of the perturbative coefficients.

Monte Carlo (MC) Simulations

- **PYTHIA:** most widely used program to generate the collisions at high energies.
 - ▶ Uses LO calculations to derive the colored partons from the hard interaction.
 - ▶ Uses the Lund string hadronization model to describe hard and soft interactions and parton showers.
 - ▶ PYTHIA6 with tune Z2* and PYTHIA8 with tunes CUETS1 and CUETM1 have been used.
- **MADGRAPH :** generates LO matrix elements for high energy physics processes.
 - ▶ Stores the event information of the particles in the Les Houches format.
 - ▶ MADGRAPH5 has been interfaced to PYTHIA6 with tune Z2* - used mainly for general comparisons to the data and calculating the detector resolution.
- **HERWIG (Hadron Emission Reactions With Interfering Gluons) :** a multi-purpose LO event generator.
 - ▶ Uses angular ordering for parton showers and cluster model for hadronization.
 - ▶ HERWIG++ with the default tune of version 2.3 has been used to study the non-perturbative effects.
- **POWHEG (Positive Weight Hardest Emission Generator)** : performs the fixed NLO calculations merged with parton showers.
 - ▶ Uses POWHEG BOX to implement NLO calculations in shower MC programs.
 - ▶ POWHEG has been interfaced to PYTHIA8 with tunes CUETS1 and CUETM1 to include the parton shower and hadronization.

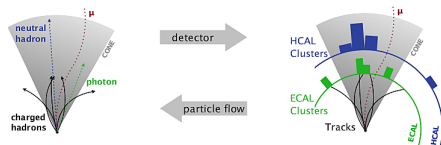
Simulation and Reconstruction

- **Detector Simulation** - a computer program which takes the particles generated by MC event generators.
 - ▶ Defines the detector system, its geometry, material and electronics properties.
 - ▶ **Full Simulation** - based on a C++ simulation toolkit GEANT4 (GEometry ANd Tracking); handles the interactions of particles with matter over a wide range of energy.
 - ▶ **Fast Simulation** - detector effects are parametrized instead of simulating; events are produced at much faster rates.
- **Digitization** : The simulated detector response is then transformed into a digital signal with the help of electronics.
- **Event Reconstruction** : identifies the particles passing through the detector by interpreting the electrical signals produced in digitization.
 - ▶ Analysis-level objects are created by combining recorded signals from the tracker, energy deposits from calorimeters and muon detectors.
 - ▶ **Particle Flow (PF) Algorithm** combines the information from individual sub-detectors.
- **Track Reconstruction** : CMS uses an iterative tracking algorithm.
 - ▶ Quality criteria is used to reject the badly reconstructed tracks and to decrease the fake rate.
- **Primary Vertex Reconstruction** : identification of the primary vertex of the main hard interaction is crucial.
 - ▶ Track assigned to only one vertex → **hard interaction**.
 - ▶ Track assigned to more than one vertex → **soft interaction**.

Jet Reconstruction

- PF event reconstruction algorithm converts the detector signals back to physical objects and their energy is measured :

- Electrons** : from the track momentum, corresponding ECAL energy deposits and the energy sum of all bremsstrahlung photons associated with the tracks.
- Muons** : from the curvature of the tracks in tracker and muon chambers.
- Photons** : directly from the ECAL measurements.
- Charged hadrons** : from track momentum and corresponding energy clusters in ECAL and HCAL.
- Neutral hadrons** : from calibrated ECAL and HCAL energies.

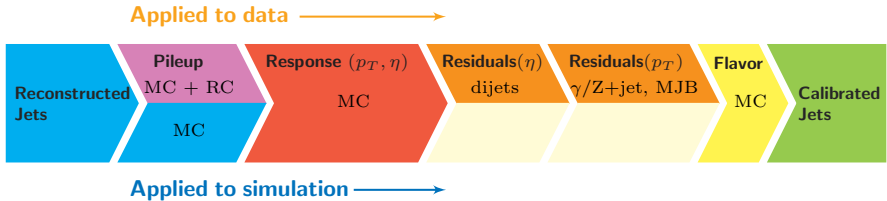


- Jets : are reconstructed from the collection of PF objects.

- Generator Jets (GenJets)**: stable particles generated by the MC event generators.
- Calorimetric Jets (CaloJets)** : energy deposits in the ECAL and HCAL towers.
- Particle Flow Jets (PFJets)** : detector level jets from particle flow candidates.
 - Use of the tracker and high granularity of the ECAL gives better energy resolution.
 - PFJets perform better than CaloJets and are the standard jets used at CMS.

Jet Energy Corrections

- The measured energy of jets cannot be directly translated to the energy at true particle or parton level. This is because of the nonlinear and nonuniform response of the calorimeters, effects of pileup and small residual effects in the data remaining after the corrections based on MC simulations. Hence the jet energy corrections (JEC) [?, ?] are used to correct the measured jet energy and relate it to the corresponding true particle jet energy. To correct the energy of jets, the CMS follows a factorized approach, as presented in Fig. 1, where JEC are applied in a sequential manner with fixed order, i.e. the output of one step serves as the input for the next one. Each level of correction takes care of a different effect and is independent of each other. At each step, the jet four-momenta is scaled with a correction factor which depends on jet p_T , η , flavor etc.



Analysis Strategy

- In a proton-proton collision, the inclusive jet cross-section studied as a function of jet properties, provides essential information about the parton distribution functions of the proton and the strong coupling constant. This chapter describes the measurement of differential inclusive multijet event cross-sections and the cross-section ratio. The event and jet selections, trigger studies, spectrum construction, corrections applied and calculation of the experimental uncertainties are discussed in detail.

The differential inclusive multijet event cross-sections, given by Eq. 2, are studied as a function of the average transverse momentum, $H_{T,2}/2 = \frac{1}{2}(p_{T,1} + p_{T,2})$, where $p_{T,1}$ and $p_{T,2}$ denote the transverse momenta of the two leading jets.

$$\sigma(H_{T,2}/2) = \frac{1}{\epsilon}$$

$L_{int,eff} \frac{N_{event}}{\Delta(H_{T,2}/2)}$ (2) where N_{event} is the number of inclusive n -jet events counted in an $H_{T,2}/2$ bin, ϵ is the product of the trigger and jet selection efficiencies, which are greater than 99%, $L_{int,eff}$ is the effective integrated luminosity, and $\Delta(H_{T,2}/2)$ are the bin widths which increase with $H_{T,2}/2$ and are proportional to the $H_{T,2}/2$ resolution. The measurements are reported in units of (pb/). The inclusive n -jet event samples include the events with number of jets $\geq n$. In the present thesis, the measurements are performed for $n = 2$ giving inclusive 2-jet events ($n_j \geq 2$) and for $n = 3$ giving inclusive 3-jet events ($n_j \geq 3$). The cross-section ratio R_{32} , defined in Eq. 3 is obtained by dividing the differential cross-sections of inclusive 3-jet events to that of inclusive 2-jet one, for each bin in $H_{T,2}/2$.

$$R_{32} = \left[\frac{\sigma_{H_{T,2}/2}(H_{T,2}/2)_{n=3}}{\sigma_{H_{T,2}/2}(H_{T,2}/2)_{n=2}} \right] \quad (3)$$

Definition of Observable

- Theoretical results suggest to use a dynamical scale based on the total transverse momentum of the jets, $H_{T,n}$ (with $n = \text{no. of jets}$) which is defined as :

$$\frac{H_{T,n}}{2} = \frac{\sum_{i=1}^n p_{T,i}}{2}$$

- In the current study, the scale used is :

$$\frac{H_{T,2}}{2} = \frac{\sum_{i=1}^2 p_{T,i}}{2}$$

which is same as $\langle p_{T,1,2} \rangle$ as used for R_{32} at 7 TeV.

Samples used :

- The measurement is performed using a sample of multijet events, collected during **2012** by the CMS experiment at the Large Hadron Collider (LHC), corresponding to total luminosity **19.71 fb⁻¹** of pp collisions at the center of mass energy $\sqrt{s} = 8 \text{ TeV}$.
- To do the Data-Monte Carlo Comparison, **MadGraph+Pythia6 Summer12 MC** sample for 8 TeV is used.
- Theoretical **NLO** (Next-to-leading order) calculations are computed with the **NLOJET++** program using PDF **CT10nlo** ($\alpha_S(M_Z) = 0.118$) are available for 2+ and 3+ jet cross-sections whereas for 4+ and 5+ with **Sherpa/Njet/mcgrid** are in preparation.

Work Flow

Tasks done :

- Jet Reconstruction : Jets are reconstructed from particle flow objects using the **anti-k_T** clustering algorithm with the size parameter **R = 0.7**
- Event Selection : Appropriate selection criteria has been designed for choosing the best event for analysis. This measurement uses jets with $p_T > 150 \text{ GeV}$ and $|y| < 2.5$
- Pile-up re-weighting.
- Detector level comparison of differential cross-section in terms of above defined observable for full Data, MC and Theory predictions.
- Evaluated cross-section ratio, R_{32}
- Unfolding set-up and the measured cross-sections are corrected for detector smearing effects by using the Unfolding technique.
- Evaluated experimental and systematic uncertainties from different sources.
- Included results from PDF sets and calculated theoretical uncertainties.

Tasks to do :

- To add the results from other Monte Carlo (MC) generators.
- to extract the value of α_S by fitting cross-sections as well as cross-section ratio, R_{32}
- To get the analysis approved in CMS Collaboration and to make the results public.

Datasets & MC Samples

● Data :

- ▶ Full **2012** dataset collected by CMS with single jet triggers
- ▶ Integrated Luminosity : **19.7 fb⁻¹**

Run	Run Range	Dataset	Luminosity
A	190456-193621	/Jet/Run2012A-22Jan2013-v1/AOD	0.88 fb ⁻¹
B	193834-196531	/Jet[Mon,HT]/Run2012B-22Jan2013-v1/AOD	4.49 fb ⁻¹
C	198022-203742	/Jet[Mon,HT]/Run2012C-22Jan2013-v1/AOD	7.06 fb ⁻¹
D	203777-208686	/Jet[Mon,HT]/Run2012D-22Jan2013-v1/AOD	7.37 fb ⁻¹

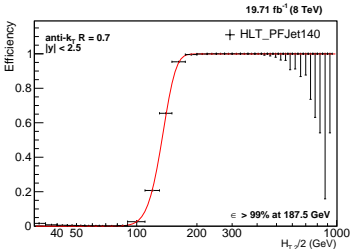
- ▶ CMS software : CMSSW_5_3_11
- ▶ JECs : Winter14_V8
- ▶ Json file: Cert_190456-208686_8TeV_22Jan2013ReReco_Collisions12_JSON.txt

● Simulated Monte-Carlo (MC) Samples :

- ▶ **MadGraph5+ Pythia6 TuneZ2* (MG+ P6 Z2*) :**
[/QCD_HT-xxxxxx_TuneZ2star_8TeV-madgraph-pythia6/Summer12_DR53X-PU_S10_START53_V7A-v1/AODSIM](#)
- ▶ **Herwig+ + Flat :**
[/QCD_Pt-15to3000_TuneEE3_Flat_8TeV_herwigpp/Summer12_DR53X-PU_S10_START53_V7A-v1/AODSIM](#)
- ▶ **Pythia6 Flat :**
[/QCD_Pt-15to3000_TuneZ2star_Flat_8TeV_pythia6/Summer12_DR53X-PU_S10_START53_V7A-v1/AODSIM](#)

- Theoretical **NLO** (Next-to-leading order) calculations using the NLOJet+ + program (v4.1.3) within the framework of the fastNLO package (v2.3) using different PDF sets

- Five single-jet high-level triggers
- Only highest-threshold trigger is unprescaled
- The trigger efficiency for HLT_PFJetY is defined as :



- the value of X is chosen previous to that of Y in p_T ordering
- Z is the L1 seed value corresponding to the trigger path
- Trigger regions defined as ranges of the $H_{T,2}/2$ for every single-jet trigger used :

PAS

HLT path	$H_{T,2}/2$ range (GeV)	Integrated Luminosity (pb^{-1})
PF Jet80	120 – 188	2.12

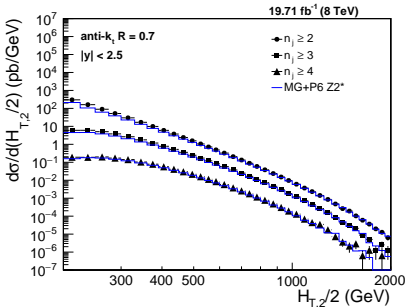
Event Selection

- anti- k_t particle flow (PF) jets with $R = 0.7$
- At least one good primary vertex : $|z(PV)| < 24 \text{ cm}$, $\rho(PV) < 2 \text{ cm}$, $ndof > 4$
- Tight jet ID criteria on each jet
- $p_T > 150.0 \text{ GeV}$ and $|y| < 5.0$
- Select events with at least two jets such that the two leading jets, which define $H_{T,2}/2$, have $|y| < 2.5$. Finally count all jets with $|y| < 2.5$
- $\frac{E_T^{\text{miss}}}{\sum E_T} < 0.3$ to protect against mismeasured or background events with large missing E_T

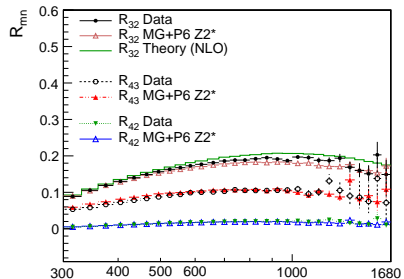
Detector Level Comparisons

- Data are compared to the sample of MG+ P6 Z2* simulated events

- ▶ LO MC generator roughly describes the spectrum on detector level



- Cross-section ratio : $R_{mn} = \frac{\sigma_{m\text{-jet}}}{\sigma_{n\text{-jet}}}$
- ▶ Numerator and denominator are not independent samples.
- ▶ To calculate the statistical uncertainty before unfolding, the **Wilson score interval** is used which takes into account the correlation between the numerator and the denominator



Jet Energy Resolution (JER)

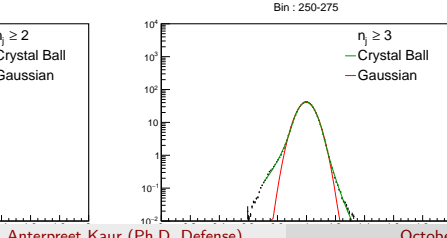
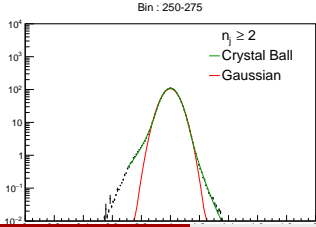
- Computed the jet energy resolution (JER) as a function of $H_{T,2}/2$ from MG+ P6 Z2* MC sample
- Measurements show that JER in data is worse than in the simulation and the jet p_T in MC need to be smeared more to describe the data
- Scaling procedure : Scaled reco jets to match resolution of data

$$p_T \rightarrow \max[0., \text{gen} + c * (p_T - \text{gen})]$$

- Non-gaussian tails are also scaled using same scaling factors determined for Gaussian core which leads to large response shifts for tails
- Smearing procedure : Smear the reconstructed jet p_T using a gaussian width widened by the scaling factor (c) (as followed in **SMP-16-011**)

$$p_T \rightarrow \text{Gauss}(\mu =, \sigma = (\sqrt{c^2 - 1}) \times \text{JER}^{\text{MC}})$$

- Crystal Ball Fit of Reco $H_{T,2}/2$ /Gen $H_{T,2}/2$ in each Gen $H_{T,2}/2$ bin overlayed by Gaussian fit

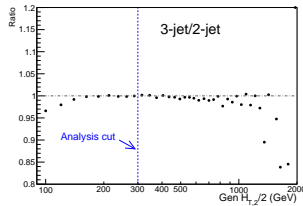
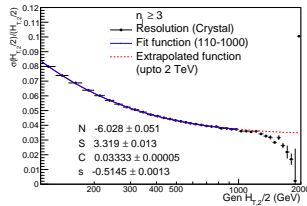
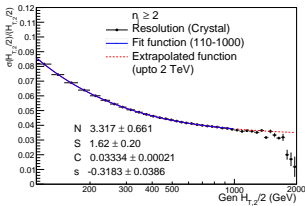


Jet Energy Resolution (JER)

- Fit using NSC-formula (adapted for PF jets)

$$\frac{\sigma(x)}{x} = \sqrt{\text{sgn}(N) \cdot \frac{N^2}{x^2} + \frac{S^2}{x} \cdot x^s + C^2}$$

- Fits at high $H_{T,2}/2$ start lacking events

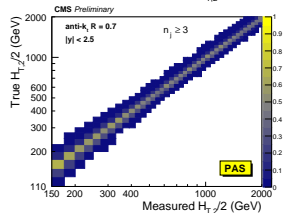
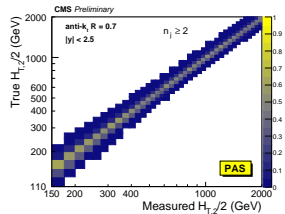


	N	S	C	s
Inclusive 2-jet	3.32	1.62	0.0333	-0.318
Inclusive 3-jet	-6.03	3.32	0.0333	-0.515

- Resolution is similar in inclusive 3-jet and 2-jet (Right Fig.)
- Fit parameters are used for smearing of NLO spectrum to construct response matrices

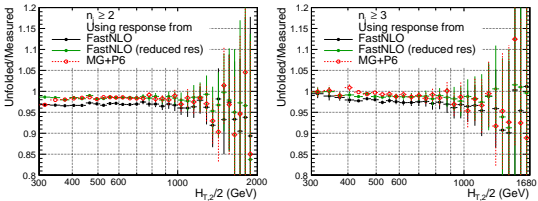
Unfolding

- Differential multijet cross-sections are corrected for smearing effects and unfolded to particle level
- Unfolding is performed using the iterative D'Agostini method with **4 iterations**, implemented in the RooUnfold software package
- Other number of iterations looked at (Slide no. 60 in Back-Up)
- Response matrices are shown
 - diagonal in nature, which are constructed using the Toy MC
 - Fit the NLO $H_{T,2}/2$ spectrum by the following function to obtain the true distributions (more details in Back-Up slide no. 57)
- $$f(p_T) = N[x_T]^{-a}[1 - x_T]^b \times \exp[-c/x_T]$$
- The smeared distributions are generated by taking into account the additionally smeared MC resolution.
- Closure tests : small non-closures observed, accounted for additional uncertainty (more details in Back-Up slide no. 62)

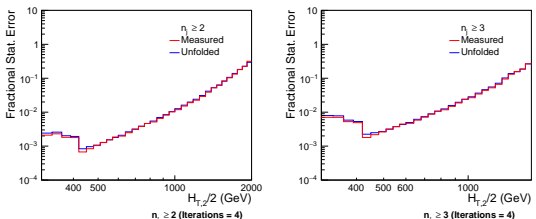


Unfolding cross-sections

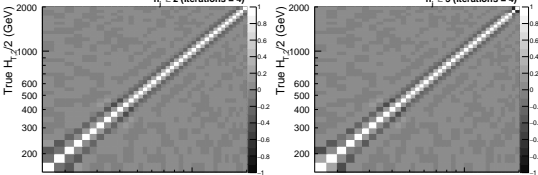
- Ratio of the unfolded data to the measured data with $H_{T,2}/2 > 300$ GeV



- Statistical errors in the unfolded distributions are slightly higher

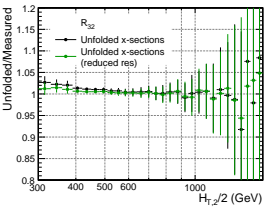


- Correlation of the statistical uncertainty introduced by the unfolding procedure

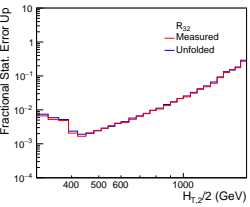


Unfolding R_{32}

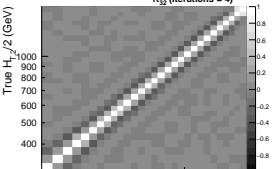
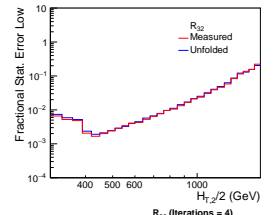
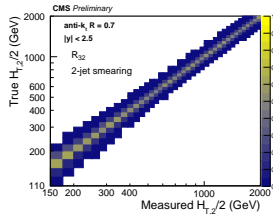
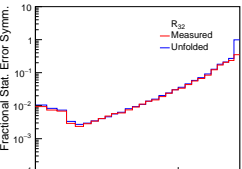
- Ratio of the unfolded cross-sections gives unfolded R_{32}



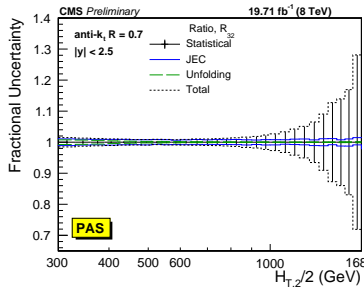
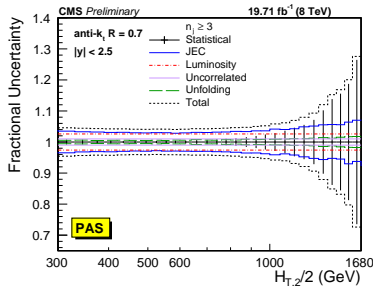
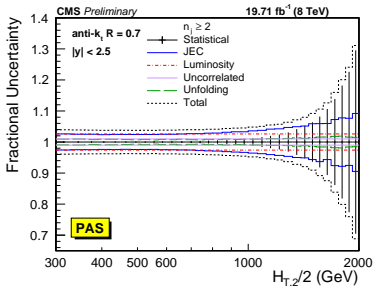
- Only to calculate the statistical correlations, R_{32} is unfolded directly using ToyMC method.



- Correlation of the statistical uncertainty introduced by the unfolding procedure



Experimental uncertainties



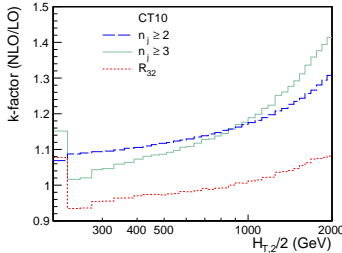
Uncertainty Source	Inclusive 2-jet	Inclusive 3-jet	R_{32}
Statistical	< 1 to 30%	< 1 to 30%	< 1 to > 50%
JEC	3 to 10%	3 to 8%	1 to 2%
Unfolding	1 to 2%	1 to 2%	1%
Luminosity	2.6%	2.6%	cancels
Residual			
uncorrelated	1%	1%	cancels

Unfolding systematic uncertainty :

- ▶ JER uncertainty : varying scale factors
- ▶ Additional uncertainty : 30% reduced resolution
- ▶ Model dependence : different functions to fit NLO distributions

Next-to-leading order (NLO) Calculations

- The NLO theoretical calculations are done using the parton-level generator NLOJet+ + within the fastNLO framework.
- The renormalization and factorization scales (μ_r and μ_f) are equal to $H_{T,2}/2$.
- Used different PDF sets (details on next slide)
- Uncertainties due to renormalization and factorization are evaluated by varying the default scale $H_{T,2}/2$ chosen for μ_r and μ_f independently in the following six combinations $(\mu_r/H_{T,2}/2, \mu_f/H_{T,2}/2) = (1/2, 1/2), (1, 1/2), (1/2, 1), (1, 2), (2, 1)$ and $(2, 2)$
- k-factor is calculated as : $k_{\text{fac}} = \frac{\sigma_{\text{NLO}}}{\sigma_{\text{LO}}}$, $k_{\text{fac}} R_{32} = \frac{k_{\text{fac}}^{\text{3-jet}}}{k_{\text{fac}}^{\text{2-jet}}}$



- kfactor jumps at lowest $H_{T,2}/2$ for inclusive 3-jet events : Below 225 GeV some jet configurations are kinematically forbidden and the first few bins shown still suffer from these kinematical effects

Details on PDF sets

- Investigated PDF sets available via LHAPDF6

PAS

Base set	N_F	M_t (GeV)	M_Z (GeV)	$\alpha_S(M_Z)$	$\alpha_S(M_Z)$ range
ABM11	5	180	91.174	0.1180	0.110–0.130
CT10	≤ 5	172	91.188	0.1180*	0.112–0.127
MSTW2008	≤ 5	10^{10}	91.1876	0.1202	0.110–0.130
NNPDF2.3	≤ 6	175	91.1876	0.1180*	0.114–0.124
CT14	≤ 5	172	91.1876	0.1180*	0.113–0.123
HERAPDF2.0	≤ 5	173	91.1876	0.1180*	0.110–0.130
MMHT2014	≤ 5	10^{10}	91.1876	0.1180*	0.108–0.128
NNPDF3.0	≤ 5	173	91.2	0.1180*	0.115–0.121

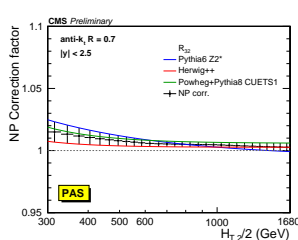
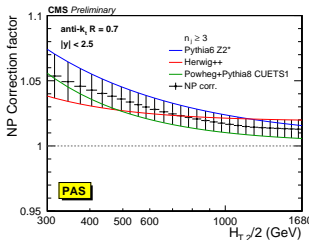
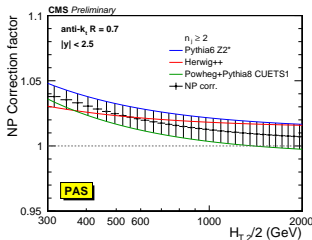
A * behind the $\alpha_S(M_Z)$ values signifies that the parameter was fixed, not fitted

- Out of these eight PDF sets the following three will not be considered further :
 - ABM11 : do not describe LHC jet data at small jet rapidity
 - HERAPDF2.0 : exclusively fits HERA DIS data with only weak constraints on the gluon PDF
 - NNPDF3.0 : the range in values available for $\alpha_S(M_Z)$ is too limited
- MSTW2008, MMHT2014 : $10^{10} \rightarrow$ Five flavours, with top quark mass \approx infinity

Non-Perturbative (NP) Corrections

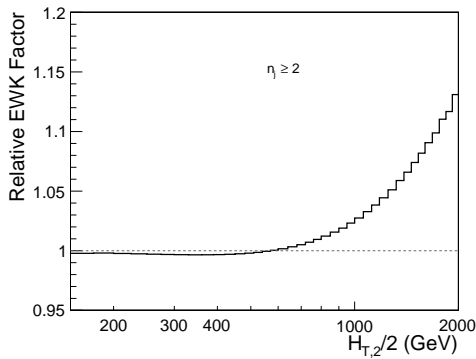
- NP corrections are required to the NLO spectrum, to compare with the experimental measurement.
 - LO generators : Pythia6 Z2* and Herwig++ (tune 2.3)
 - NLO generator : Powheg+ Pythia8 CUETS1
- NP factor is obtained by switching MPI and hadronization on/off, $c^{\text{NP}} = \frac{\sigma^{\text{PS+ HAD+ MPI}}}{\sigma^{\text{PS}}}$
- Mean value of the envelope taken gives the NP factor and the envelope covering all differences taken as uncertainty.
- For R_{32} : first the ratio of cross sections of inclusive 3-jet to that of 2-jet events are taken separately for hadronization and MPI effects switched off and on. Then the ratio defined above is used to calculate the NP correction factor.

$$c_{R_{32}}^{\text{NP}} = \frac{\left(\frac{\sigma_{\text{3-jet}}}{\sigma_{\text{2-jet}}} \right)^{\text{PS+HAD+MPI}}}{\left(\frac{\sigma_{\text{3-jet}}}{\sigma_{\text{2-jet}}} \right)^{\text{PS}}}$$

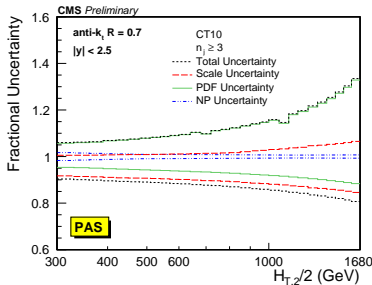
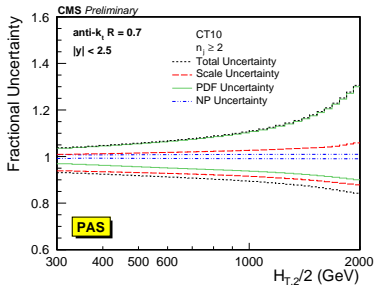


Electroweak Corrections (EWK)

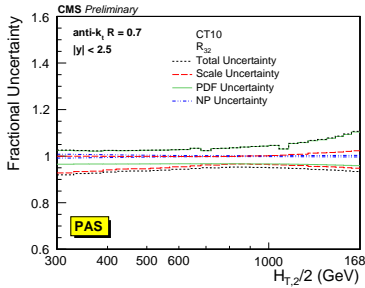
- EWK account for contributions from electroweak bosons
- Only available for inclusive 2-jet
- Best guess from theory :
 - ▶ EWK similar for inclusive 2-jet and 3-jet and hence factor of 1 for R_{32}



Theoretical Uncertainties



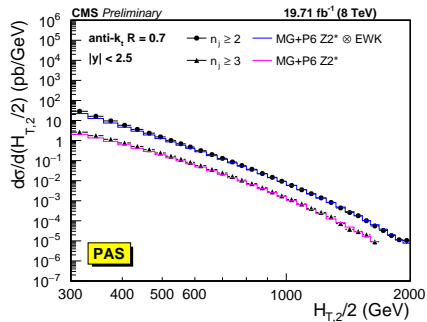
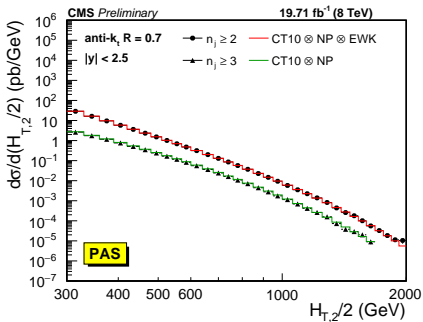
Uncertainty Source	Inclusive 2-jet	Inclusive 3-jet	R ₃₂
Scale	5 to 13%	11 to 17%	6 to 8%
PDF	2 to 30%	2 to 30%	2 to 7%
NP	4 to 5%	4 to 5%	1%



- Small dips at 1.X TeV in the PDF uncertainty (top right) : It is a feature of the CT10 PDF. Likewise the smaller dip at 700 GeV. If another PDF, e.g. CT14, is used, these dips are gone (Slide no. 70 in Back-Up).

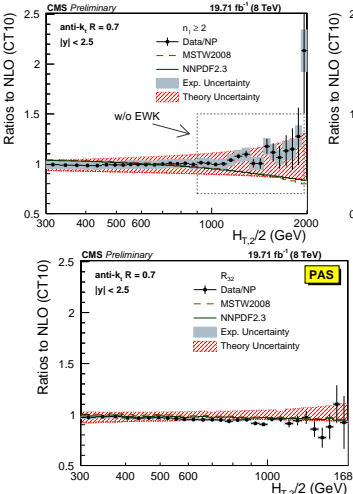
Inclusive Differential Multijet Measurement

- Inclusive differential multijet cross sections are measured as a function of the average transverse momentum, $H_{T,2}/2$
 - On Left :** NLOJet+ + predictions based on the CT10 PDF set and corrected for NP effects, in addition for EWK effects in the 2-jet case
 - predictions are compatible with data within uncertainties over a wide range of $H_{T,2}/2$ from 300 GeV up to 2 TeV
 - On Right :** predictions from MG+ P6 Z2*, corrected for EWK effects in the 2-jet case
 - significant discrepancies are visible in the ratio for comparison with the leading-order (LO) tree-level prediction



Comparison with NLO Predictions - CT10

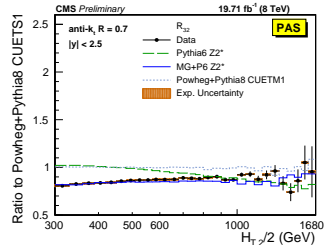
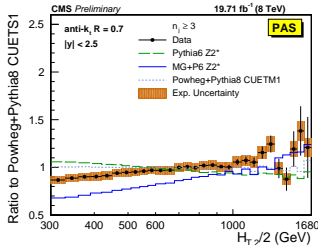
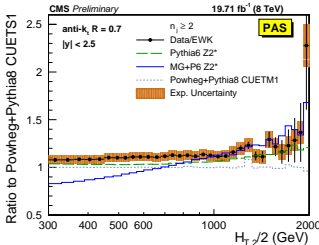
- Ratio to NLO \otimes NP \otimes EWK - CT10
- Data points with statistical uncertainty
- Theoretical uncertainty : quad. sum of scale, NP and PDF uncertainties



- Electroweak corrections explain the increasing systematic excess of data with respect to theory beyond 1 TeV of $H_{T,2}/2$ for inclusive 2-jet (Left and Middle figures)
- For brevity, the relative factor of NP between data and theory has been indicated as "Data/NP" in the legend

Comparison with MC Generators

- Ratios to Powheg+ Pythia8 tune CUETS1
- Data points with statistical uncertainty
- Experimental uncertainty shows total systematic uncertainty
- Comparison with
 - ▶ LO prediction from MG+ P6 Z2* and tree-level multi-leg improved prediction by Pythia6 Z2* : Significant discrepancies, which are cancelled to a large extent in the ratio R_{32} , are visible in particular for small $H_{T,2}/2$
 - ▶ with the matched dijet NLO prediction from Powheg+ Pythia8 with tune CUETM1 : better describes the 2-jet event cross section, but fails for the 3-jet case.

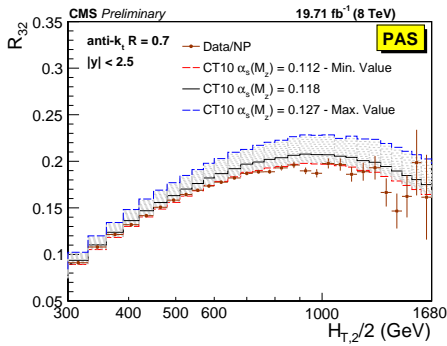


Cross section ratio (R_{32})

- The cross-section ratio R_{32} as a function of $H_{T,2}/2$ is extracted by dividing the differential cross section for inclusive 3-jet over 2-jet events for each bin in $H_{T,2}/2$

$$R_{32} = \frac{\sigma_{\text{3-jet}}}{\sigma_{\text{2-jet}}} \propto \alpha_S$$

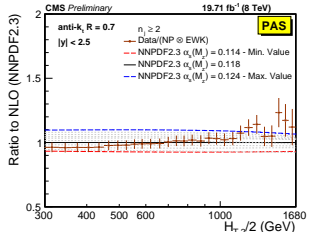
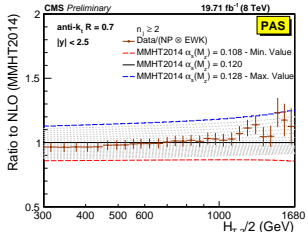
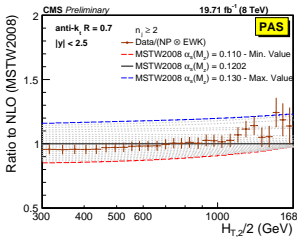
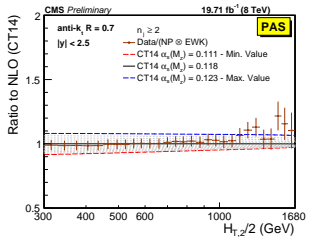
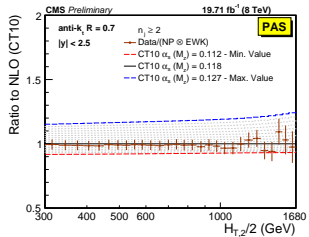
- R_{32} obtained from unfolded data in comparison to that from CT10 NLO with NP corrections. The error bars correspond to the total experimental uncertainty.



- The other ratios will also be included once the theory predictions for inclusive 4-jet events are available (for Paper).

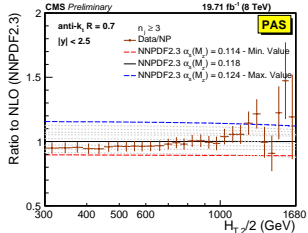
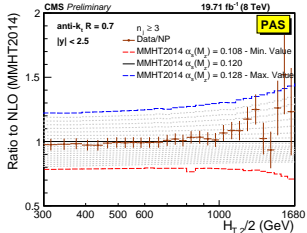
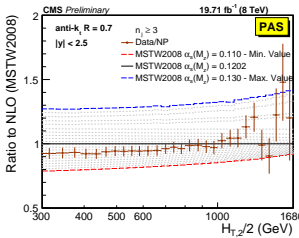
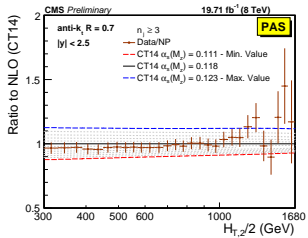
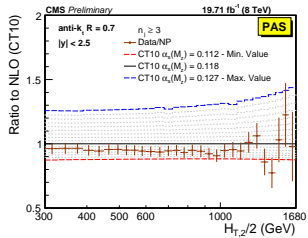
Sensitivity of differential inclusive 2-jet cross section to $\alpha_S(M_Z)$

- $\sigma_{2\text{-jet}} \propto \alpha_S^2$



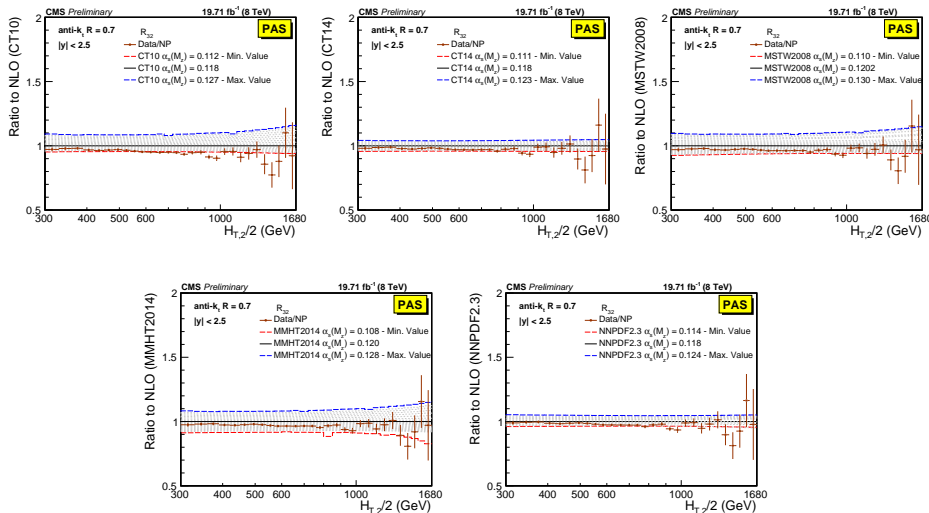
Sensitivity of differential inclusive 3-jet cross section to $\alpha_s(M_z)$

- $\sigma_{3\text{-jet}} \propto \alpha_s^3$



Sensitivity of R_{32} to $\alpha_s(M_z)$

$$R_{32} \propto \alpha_S^1$$



Determination of the Strong Coupling Constant

- Fit of α_S using χ^2 similar to recipe as used by previous R_{32} @ 7 TeV and inclusive jets @ 8 TeV analysis

$$\chi^2 = M^T C^{-1} M$$

$$M^i = D^i - T^i$$

- $C = C_{\text{exp}} + C_{\text{theo}}$ is defined as the sum of covariances of experimental and theoretical sources of uncertainty as follows :

$$C_{\text{exp}} = \text{Cov}^{\text{ExpStat}} + \sum \text{Cov}^{\text{JEC}} + \text{Cov}^{\text{Unfolding}} + \text{Cov}^{\text{Lumi}} + \text{Cov}^{\text{Uncor}}$$

$$C_{\text{theo}} = \text{Cov}^{\text{TheoStat}} + \text{Cov}^{\text{NP}} + \text{Cov}^{\text{PDF}}$$

- $\text{Cov}^{\text{ExpStat}}$: the statistical uncertainty of the data including correlations introduced by the unfolding,
 - Cov^{JEC} : the JEC systematic uncertainty,
 - $\text{Cov}^{\text{Unfolding}}$: the unfolding systematic uncertainty including the JER,
 - Cov^{Lumi} : the luminosity uncertainty,
 - $\text{Cov}^{\text{Uncor}}$: a residual uncorrelated systematic uncertainty summarizing individual causes such as trigger and identification inefficiencies, time dependence of the jet p_T resolution, and uncertainty on the trigger prescale factors,
 - $\text{Cov}^{\text{TheoStat}}$: the statistical uncertainty caused by numerical integrations in the cross section computations,
 - Cov^{NP} : the systematic uncertainty of the NP corrections, and
 - Cov^{PDF} : the PDF uncertainty.
- For the fits of the cross sections, the range in $H_{T,2}/2$ is restricted to be between 300 GeV and 1 TeV : to avoid the region close to the minimal p_T threshold of 150 GeV for each jet at low p_T and the onset of electroweak effects at high p_T

Fit results in range $0.3 < H_{T,2}/2 < 1.00$ TeV

PAS

PDF set	2-jets			3-jets		
	$\alpha_S(M_Z)$	$\pm \Delta \alpha_S(M_Z)$	χ^2/n_{dof}	$\alpha_S(M_Z)$	$\pm \Delta \alpha_S(M_Z)$	χ^2/n_{dof}
CT10	0.1174	0.0032	3.0/18	0.1169	0.0027	5.4/18
CT14	0.1160	0.0035	3.5/18	0.1159	0.0031	6.1/18
MSTW2008	0.1159	0.0025	5.3/18	0.1161	0.0021	6.7/18
MMHT2014	0.1165	0.0034	5.9/18	0.1166	0.0025	7.1/18
NNPDF2.3	0.1183	0.0025	9.7/18	0.1179	0.0021	9.1/18

ignored correlations			accounted for correlations			PAS	
PDF set	2- & 3-jets		$\alpha_S(M_Z)$	$\pm \Delta \alpha_S(M_Z)$	χ^2/n_{dof}		
	$\alpha_S(M_Z)$	$\pm \Delta \alpha_S(M_Z)$					
CT10	0.1170	0.0026	8.2/37	0.1141	0.0028	19./18	
CT14	0.1161	0.0029	9.1/37	0.1139	0.0032	15./18	
MSTW2008	0.1161	0.0021	11./37	0.1150	0.0023	21./18	
MMHT2014	0.1168	0.0025	11./37	0.1142	0.0022	19./18	
NNPDF2.3	0.1188	0.0019	15./37	0.1184	0.0021	12./18	

- All cross section fits give compatible values for $\alpha_S(M_Z)$ in the range of 0.115 - 0.118
- For R_{32} , smaller values are obtained as in the previous CMS R_{32} publication [Eur. Phys. J. C 73 (2013) 2604]
- small χ^2/n_{dof} except for the R_{32} fits : may be due to an overestimation of the residual uncorrelated uncertainty of 1% that is cancelled for R_{32} .
- With an assumed uncertainty of 0.25% : the χ^2/n_{dof} values lie around unity while the $\alpha_S(M_Z)$ values are still compatible with the previous results but with slightly reduced

Fit results in range $0.3 < H_{T,2}/2 < 1.68$ TeV

- $\alpha_S(M_Z)$ fits to the 2-jet event cross section with or without EWK correction factors.
 - ▶ Reduction in χ^2/n_{dof} indicating a better agreement when EWK effects are included.
 - ▶ A tendency to slightly smaller $\alpha_S(M_Z)$ values is observed without the EWK corrections.

PAS

PDF set	2-jets, without EWK			2-jets, with EWK		
	$\alpha_S(M_Z)$	$\pm \Delta \alpha_S(M_Z)$	χ^2/n_{dof}	$\alpha_S(M_Z)$	$\pm \Delta \alpha_S(M_Z)$	χ^2/n_{dof}
CT10	0.1163	0.0034	15./28	0.1165	0.0032	14./28
CT14	0.1137	0.0033	24./28	0.1144	0.0033	17./28
MSTW2008	0.1093	0.0028	27./28	0.1133	0.0023	19./28
MMHT2014	0.1127	0.0032	32./28	0.1141	0.0032	21./28
NNPDF2.3	0.1162	0.0024	31./28	0.1168	0.0024	23./28

- Results from the two most compatible PDF sets MSTW2008 and MMHT2014 at NLO :
 - ▶ provide a large enough range in $\alpha_S(M_Z)$ values to ensure fits without extrapolation
 - ▶ Other three PDF sets are at the limit such that reliable fits cannot be performed for estimation of all uncertainties.

PAS

PDF set	$\alpha_S(M_Z)$	R ₃₂ : $\Delta \alpha_S(M_Z) \times 1000$					
		exp	PDF	NP	all exc.	scale	χ^2/n_{dof}
MSTW2008	0.1150	± 10	± 13	± 15	± 23	$+50$ -0	26./28
MMHT2014	0.1142	± 10	± 13	± 14	± 22	$+49$ -6	24./28

Fit results in range $0.3 < H_{T,2}/2 < 1.68$ TeV

- Using R_{32} at the central scale and for the six scale factor combinations for the two PDF sets MSTW2008 and MMHT2014

PAS

$\mu_r/H_{T,2}/2$	$\mu_f/H_{T,2}/2$	MSTW2008		MMHT2014	
		$\alpha_S(M_Z)$	χ^2/n_{dof}	$\alpha_S(M_Z)$	χ^2/n_{dof}
1	1	0.1150	26./28	0.1142	24./28
1/2	1/2	0.1165	77./28	0.1160	73./28
2	2	0.1120	18./28	0.1191	18./28
1/2	1	0.1150	53./28	0.1136	48./28
1	1/2	0.1150	30./28	0.1142	28./28
1	2	0.1155	23./28	0.1147	22./28
2	1	0.1180	19./28	0.1175	19./28

- Uncertainty composition for $\alpha_S(M_Z)$ from the determination of α_S in bins of $H_{T,2}/2$

PAS

$H_{T,2}/2$ (GeV)	$\alpha_S(M_Z)$	MSTW2008: $\Delta\alpha_S(M_Z) \times 1000$			MMHT2014: $\Delta\alpha_S(M_Z) \times 1000$				
		exp	PDF	NP	scale	exp	PDF	NP	scale
300–420	0.1157	± 15	± 14	± 19	+53 -0	0.1158	± 14	± 10	± 19 +52 -0
420–600	0.1153	± 11	± 14	± 18	+57 -0	0.1154	± 11	± 12	± 17 +56 -0
600–1000	0.1134	± 13	± 16	± 19	+52 -0	0.1140	± 12	± 12	± 18 +45 -0
1000–1680	0.1147	± 29	± 17	± 18	+63 -11	0.1154	± 25	± 14	± 15 +56 -11
300–1680	0.1150	± 10	± 13	± 15	+50 -0	0.1142	± 10	± 13	± 14 +49 -6

Summary

- A measurement of the inclusive 2-jet (3-jet) event cross sections has been presented in a range of $0.3 < H_{T,2}/2 < 2.0$ TeV ($0.3 < H_{T,2}/2 < 1.68$ TeV) for the average p_T of the two leading jets at central rapidity of $|y| < 2.5$
- Measured cross sections are corrected for detector effects and compared to NLO calculations
- Compared to the different PDF sets
 - ▶ Well described by calculations at NLO in pQCD complemented with NP corrections that are important at low $H_{T,2}/2$
- Compared to the different Monte Carlo generators
 - ▶ LO tree-level MC predictions exhibit significant deviations.
- $\alpha_S(M_Z)$ Determination
 - ▶ Performed fits of $\alpha_S(M_Z)$ from differential inclusive 2-jet and inclusive 3-jet event cross-sections separately and in combined fit as well as ratio R_{32} , in the range in $H_{T,2}/2$ of 0.3 TeV up to 1.00 TeV.
 - ▶ MSTW2008 and MMHT2014 PDF sets provide a large enough range in $\alpha_S(M_Z)$ values and give similar results in full range in $H_{T,2}/2$ of 0.3 TeV up to 1.68 TeV and for scale variations in this range, and also for subranges in $H_{T,2}/2$
 - ▶ Using MSTW2008 PDF set, the strong coupling constant is determined in a fit to the R_{32} measurement to :

$$\begin{aligned}\alpha_S(M_Z) &= 0.1150 \pm 0.0010 \text{ (exp)} \pm 0.0013 \text{ (PDF)} \pm 0.0015 \text{ (NP)} {}^{+0.0050}_{-0.0000} \text{ (scale)} \\ &= 0.1150 \pm 0.0023 \text{ (all except scale)} {}^{+0.0050}_{-0.0000} \text{ (scale)}\end{aligned}$$

- ▶ Agreement with the world average value of a $\alpha_S(M_Z) = 0.1181 \pm 0.0011$

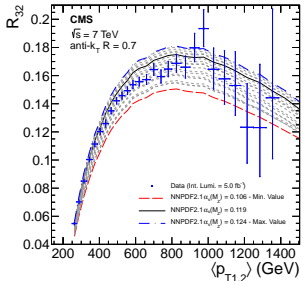
We kindly request for the approval of this analysis. Thank you !!

Back-Up Slides

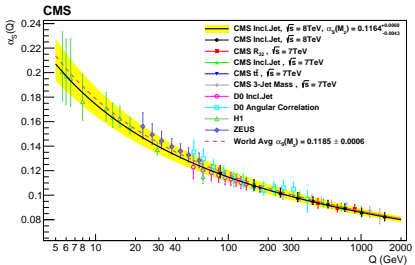
Sequential Recombination Algorithms

- Based on transverse momentum p_T of the particles.
 1. Distance d_{ij} between two particles i and j and distance d_{iB} of the particle to the beam are calculated as
$$d_{ij} = \min(p_{Ti}^{2p}, p_{Tj}^{2p}) \frac{\Delta R_{ij}^2}{R^2}, \quad d_{iB} = p_{Ti}^{2p}$$
where $\Delta R_{ij}^2 = (y_i - y_j)^2 + (\phi_i - \phi_j)^2$
 2. If $d_{ij} < d_{iB}$, particles i and j are merged into a new single jet object k , summing four-momenta of two initial particles by recombination scheme and step 1 is repeated.
 3. If $d_{iB} < d_{ij}$, particle i is declared as a final-state jet and the particle gets removed from the list.
- Value of the parameter p defines the three different sequential algorithms :
 - ▶ k_t algorithm : $p = 1$
 - ▶ Cambridge/Aachen (C/A) algorithm : $p = 0$
 - ▶ anti- k_T algorithm : $p = -1$

Previous Results



- Ratio of inclusive 3- to 2-jet events = $\frac{\sigma_{3\text{-jet}}}{\sigma_{2\text{-jet}}} \propto \alpha_S$ vs $\langle p_{T1,2} \rangle$ at $\sqrt{s} = 7 \text{ TeV}$
- Comparison with NLO calculations
- $\alpha_S(M_Z) = 0.1148 \pm 0.0014 \text{ (exp.)} \pm 0.0018 \text{ (PDF)} \pm 0.0050 \text{ (theory)} = 0.1148 \pm 0.0055$
- **7 TeV Published**
- **Eur. Phys. J. C 73 (2013) 2604**



- Measurement and QCD analysis of double-differential inclusive jet cross-sections in pp collisions at $\sqrt{s} = 8 \text{ TeV}$ and ratios to 2.76 and 7 TeV
- $\alpha_S(M_Z) \text{ (NLO)} = 0.1164^{+0.0025}_{-0.0029} \text{ (PDF)}$
 $+ 0.0053 \text{ (Scale)} \pm 0.0001 \text{ (NP)}^{+0.0014}_{-0.0015} \text{ (Exp)}$
 $= 0.1164^{+0.0060}_{-0.0043}$
- **8 TeV Submitted**
- **arXiv:1609.05331**

Introduction

- The measurement of inclusive multijet event cross-sections,

$$\sigma_{i\text{-jet}} = \sigma(pp \rightarrow i \text{ jets} + X) \propto \alpha_S^i$$

*to be fixed in text

- ▶ and their ratio

$$R_{mn} = \frac{\sigma_{m\text{-jet}}}{\sigma_{n\text{-jet}}} \propto \alpha_S^{m-n}; m > n$$

- ▶ as a function of

$$\langle p_{T,1,2} \rangle = \frac{p_{T,1} + p_{T,2}}{2} = H_{T,2}/2$$

- The inclusive differential multijet event cross section is defined as :

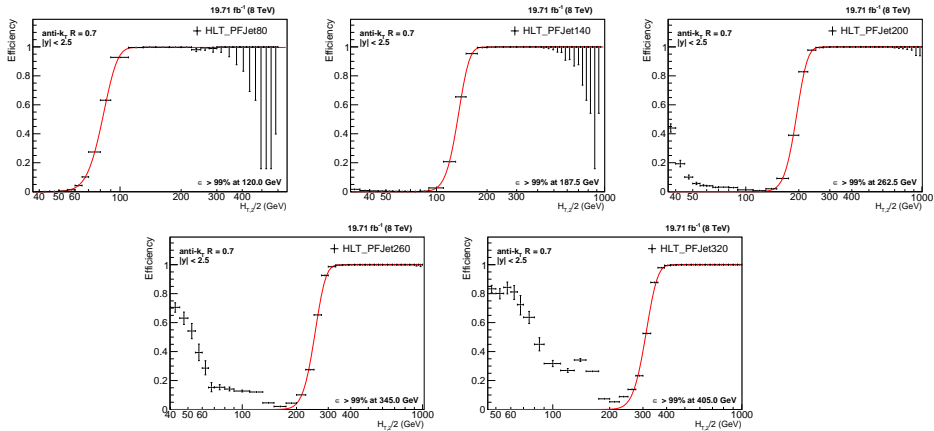
$$\frac{d\sigma}{d(H_{T,2}/2)} = \frac{1}{\epsilon \mathcal{L}_{\text{int,eff}}} \frac{N_{\text{event}}}{\Delta(H_{T,2}/2)}, \text{ where}$$

- ϵ : the product of the trigger and jet selection efficiencies and $> 99\%$,
- $\mathcal{L}_{\text{int,eff}}$: the effective integrated luminosity,
- N_{event} : the number of 2- or 3-jet events counted in an $H_{T,2}/2$ bin, and
- $\Delta(H_{T,2}/2)$: the bin widths. The measurements are reported in units of (pb/GeV) .

- The measured cross-section is corrected for detector effects and is compared to the NLO \otimes NP QCD predictions for different PDF sets
- Fits of the strong coupling constant are performed for inclusive 2-jet and 3-jet event cross-sections separately and for their ratio R_{32}
- In the talk :

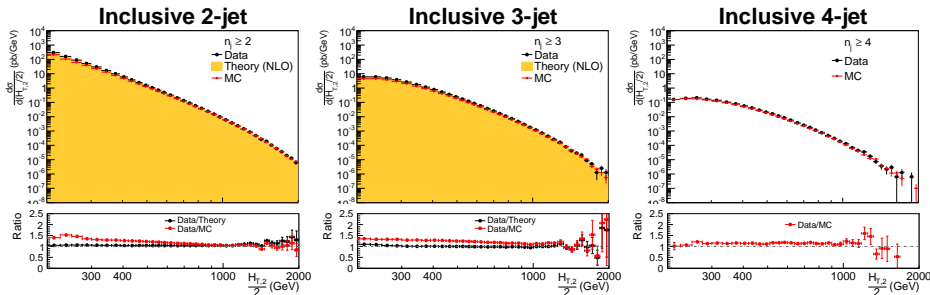
- ▶ Highlighted text in green → changed during ARC review
- ▶ Inclusive 2-jet : $n_j \geq 2$ (300–2000 GeV), Inclusive 3-jet : $n_j \geq 3$ (300–1680 GeV),
Inclusive 4-jet : $n_j \geq 4$ (only in AN for now) and ratio : R_{32} (300–1680 GeV)

Trigger Efficiencies vs $H_{T,2}/2$



Detector-Level Comparison of Cross Sections

- Binning used is inherited from R_{32} at 7 TeV : 150., 175., 200., 225., 250., 275., 300., 330., 360., 390., 420., 450., 480., 510., 540., 570., 600., 640., 680., 720., 760., 800., 850., 900., 950., 1000., 1060., 1120., 1180., 1250., 1320., 1390., 1460., 1530., 1600., 1680., 1760., 1840., 1920., 2000.
- Comparison of 2012 full data is done with NLO predictions as well as MG+ P6 MC Simulations.
- 150-200 bins are not included to avoid the infrared sensitivity for the bins next to min. p_T cut in NLO calculations for events with inclusive 2-jet events.



*NLO theory predictions are yet to be done for inclusive 4-jet events.

Unfolding : Fitting NLO predictions

- Fitting the NLO $H_{T,2}/2$ spectrum by the function (Function I)

$$f(p_T) = N[x_T]^{-a}[1 - x_T]^b \times \exp[-c/x_T]$$

where N is normalization factor and a, b, c are fit parameters.

- ▶ This function is derived from the below function from "Measurement of the Inclusive Jet Cross Section in pp Collisions at $\sqrt{s}=7$ TeV" (Phys.Rev.Lett. 107, 132001 (2011))

$$f(p_T; \alpha, \beta, \gamma) = N_0[p_T]^{-\alpha}[1 - \frac{1}{\sqrt{s}}2p_T \cosh(y_{\min})]^{\beta} \times \exp[-\gamma/p_T], \text{ where } N_0 \text{ is a normalization factor, } \alpha, \beta, \gamma \text{ are fit parameters, and } y_{\min} \text{ is the low-edge of the rapidity bin } y \text{ under consideration.}$$

using

$$\alpha = a, \quad \beta = b, \quad \gamma = c * \sqrt{s}/2,$$

$$x_T = \frac{2*p_T*cosh(y_{\min})}{\sqrt{s}} = \frac{2*p_T}{\sqrt{s}}$$

where transverse scaling variable x_T corresponds to the proton fractional momentum x for dijets with rapidity $y=0$, $\sqrt{s} = 8000$ GeV and y_{\min} is low-edge of the rapidity bin y under consideration (Here y_{\min} is taken equal to 0)

- Fitting the NLO $H_{T,2}/2$ spectrum by the function (Function II) (CMS AN-12-223) :

$$f(H_{T,2}/2) = A_0 \left(1 - \frac{H_{T,2}/2}{A_6}\right)^{A_7} \times 10^{F(x)}, \text{ where } F(x) = \sum_{i=1}^5 A_i \left(\log\left(\frac{x}{A_6}\right)\right)^i$$

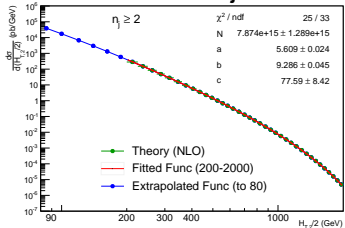
where the parameter A_6 is fixed to $\frac{\sqrt{s}}{2\cosh(y_{\min})}$, where $\sqrt{s} = 8000$ GeV and y_{\min} is the minimum rapidity. The other parameters are derived from the fitting.

Unfolding : Fitting NLO predictions

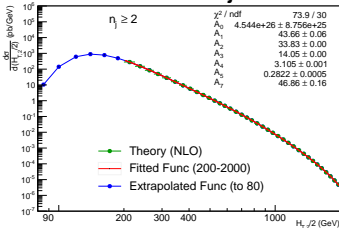
- First fit the NLO spectrum with function in the range (specified on the plot) and then using the obtained fit parameters extrapolated it to lower value.

Function I (Left) and Function II (Right)

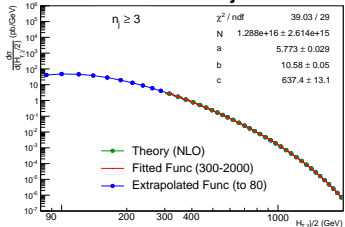
Inclusive 2-jet



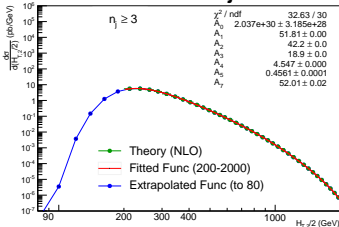
Inclusive 2-jet



Inclusive 3-jet

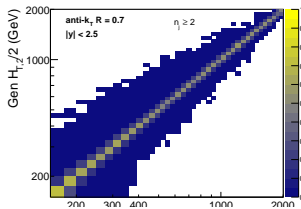


Inclusive 3-jet

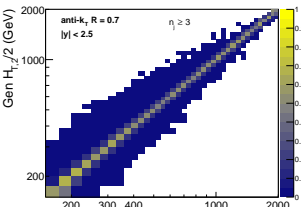


Unfolding (from MG+ P6)

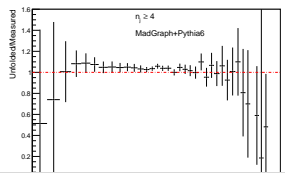
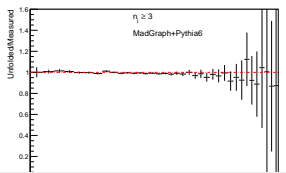
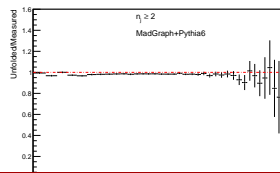
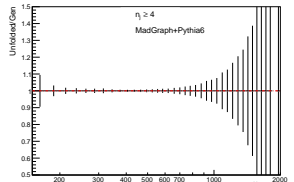
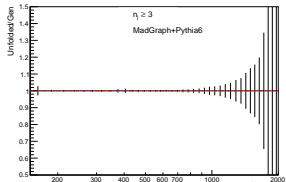
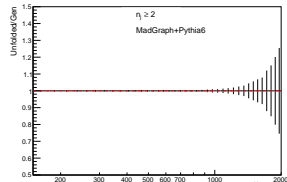
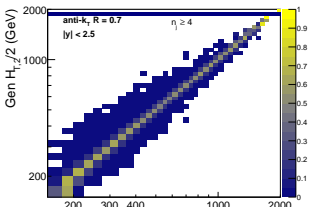
Inclusive-2 jet



Inclusive-3 jet

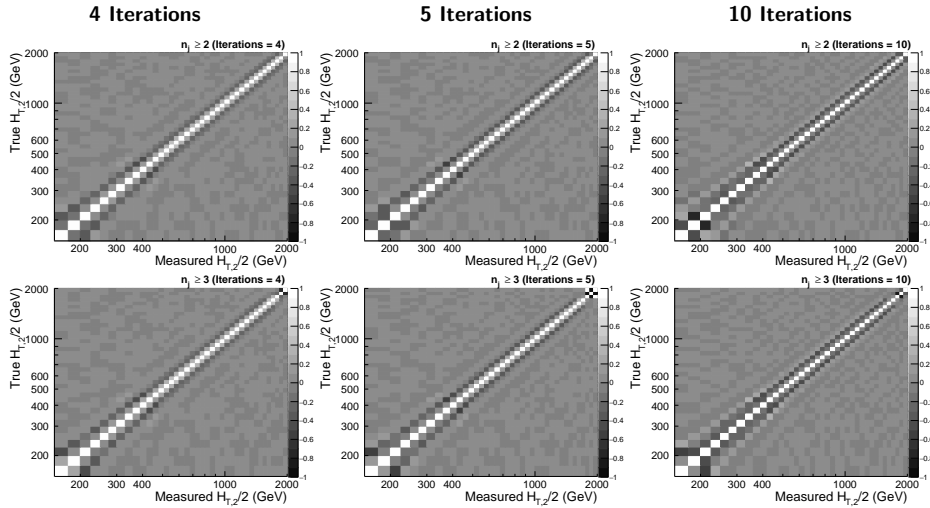


Inclusive 4-jet



Unfolding : Correlation Matrices (NLO)

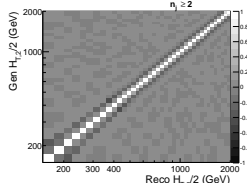
Inclusive 2-jet (Top) and Inclusive 3-jet (Bottom)



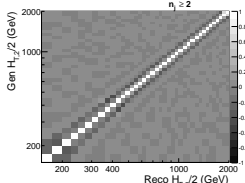
Unfolding : Correlation Matrices (MG+ P6)

Inclusive 2-jet (Top), Inclusive 3-jet (Middle) and Inclusive 4-jet (Bottom)

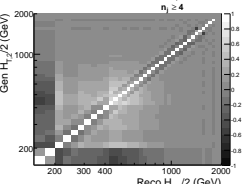
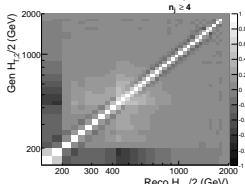
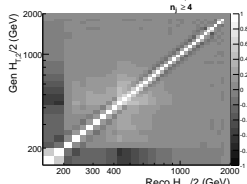
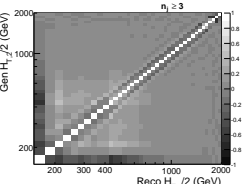
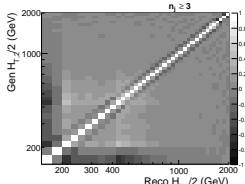
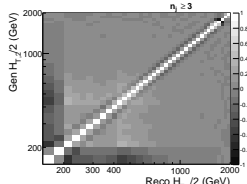
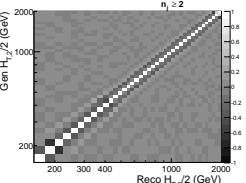
4 Iterations



5 Iterations



10 Iterations



Closure tests

- Blue curve

- Simulated MG+ P6 Reco/MG+ P6 Gen
- Resolution (Res.) is extracted from this simulation

- Red curve

- Extracted Res. smears FastNLO too much, in a very large y bin
- ARC agreed to add this non-closure as additional uncertainty for now

- Black dashed curve

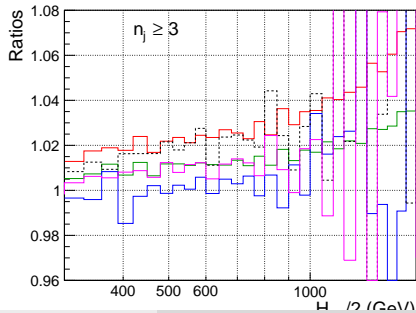
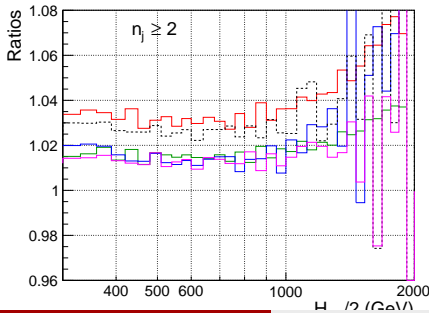
- Proves that the extracted Res. also smears MG+ P6 Gen more

- Magenta curve

- Closure with **blue curve** when 30% reduced Res. is used to smear MG+ P6 Gen

- Green curve

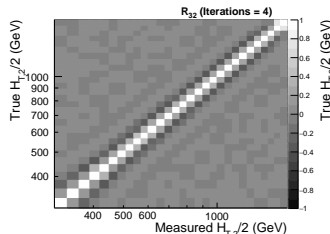
- Closure with **blue curve** when FastNLO is smeared using 30% reduced Res.
- An additional uncertainty is attributed by comparison to an unfolding with a 30% reduced Res. with the one using extracted Res.



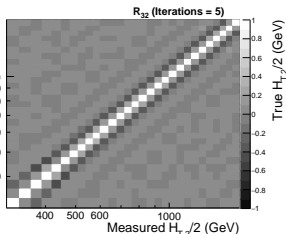
Unfolding R_{32}

Correlation Matrices (NLO)

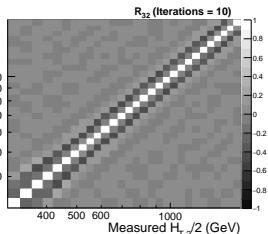
4 Iterations



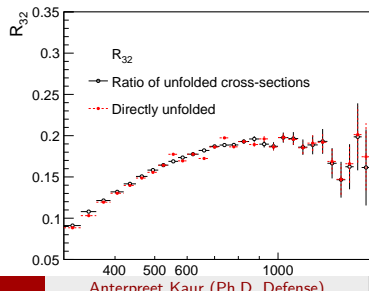
5 Iterations



10 Iterations



Unfolding R_{32}



- Jet Energy Scale (JES)

- ▶ 24 JES mutually uncorrelated uncertainty sources (Winter14_V8) are considered :
 - AbsoluteStat, AbsoluteScale, AbsoluteMPFBias,
 - Fragmentation, SinglePionECAL, SinglePionHCAL, FlavorQCD,
 - RelativeJEREC1, RelativeJEREC2, RelativeJERHF, RelativePtBB, RelativePtEC1, RelativePtEC2, RelativePtHF, RelativeFSR, RelativeStatFSR, RelativeStatEC2, RelativeStatHF,
 - PileUpDataMC, PileUpPtRef, PileUpPtBB, PileUpPtEC1, PileUpPtEC2, PileUpPtHF
- ▶ Relative uncertainties for AbsoluteFlavMap, RelativeJERHF, RelativePtHF, RelativeStatHF, PileUpPtHF are exactly zero

- To get uncertainty in P_T for each source :

double unc = Event->pfjet(p).uncSrc(isrc); where p is jet and isrc is uncertainty source

- Calculated $P_T^{\text{up}} = (1 + \text{unc}) * P_T$ and $P_T^{\text{down}} = (1 - \text{unc}) * P_T$ for each source (Event wise)

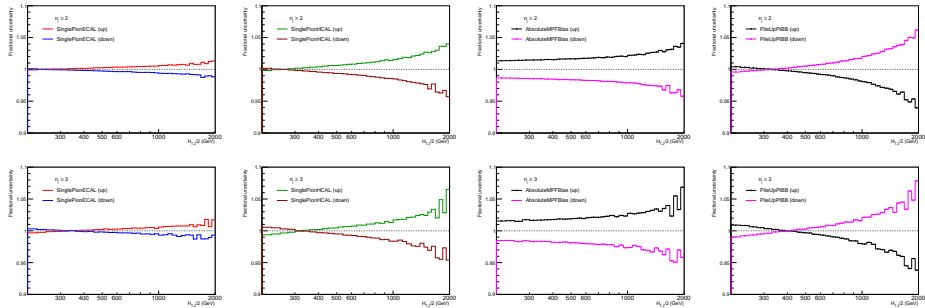
- Calculated $\frac{H_{T,2}}{2} = \frac{\sum_{i=1}^2 P_{T,i}}{2}$ and $\frac{H_{T,2}^{\text{up}}}{2} = \frac{\sum_{i=1}^2 P_{T,i}^{\text{up}}}{2}$, $\frac{H_{T,2}^{\text{down}}}{2} = \frac{\sum_{i=1}^2 P_{T,i}^{\text{down}}}{2}$ for each source (Event wise) and filled in histograms

- After filling histograms, calculated average uncertainty (%) in $\frac{H_{T,2}}{2}$, for each source :

$$\left(\frac{\frac{H_{T,2}^{\text{up}}}{2} - \frac{H_{T,2}^{\text{down}}}{2}}{2 * \frac{H_{T,2}}{2}} \right) * 100$$

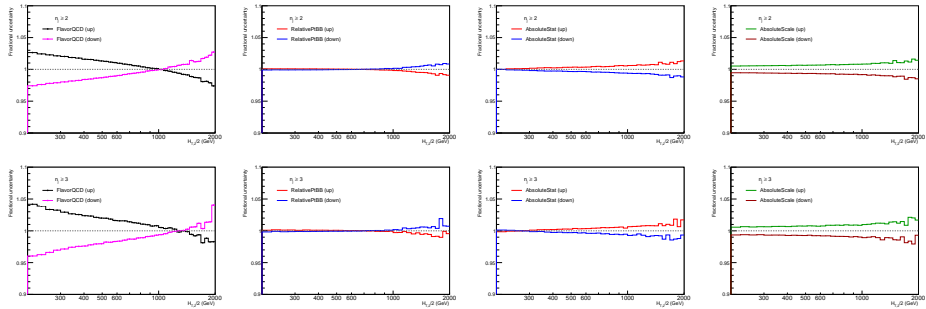
JES Uncertainty in $H_{T,2}/2$ (Single)

Inclusive 2-jet (Top) and Inclusive 3-jet (Bottom)



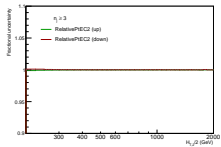
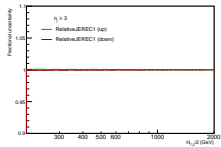
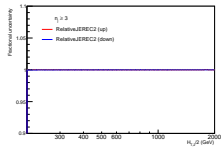
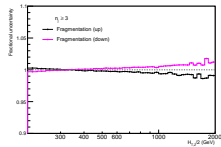
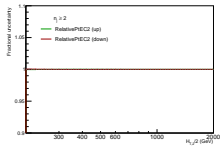
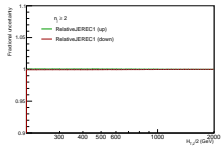
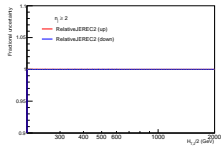
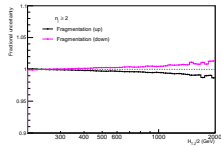
JES Uncertainty in $H_{T,2}/2$ (Single)

Inclusive 2-jet (Top) and Inclusive 3-jet (Bottom)



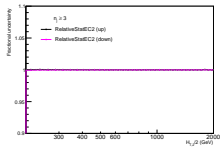
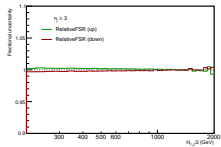
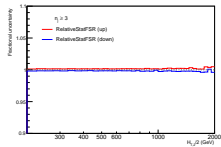
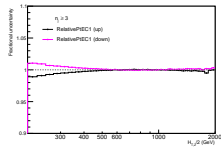
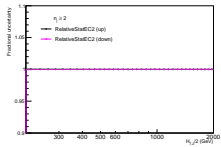
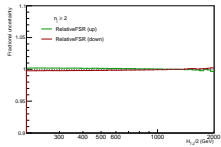
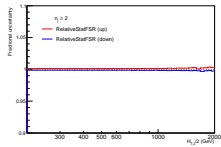
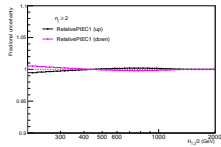
JES Uncertainty in $H_{T,2}/2$ (Single)

Inclusive 2-jet (Top) and Inclusive 3-jet (Bottom)



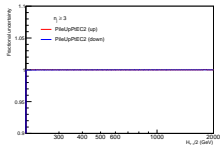
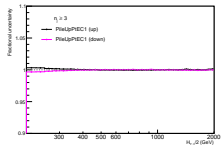
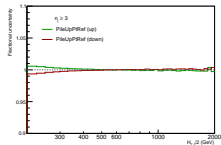
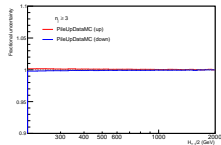
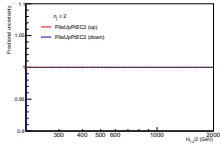
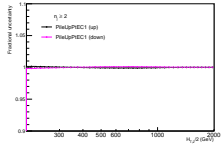
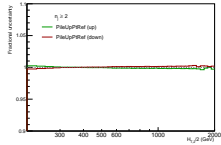
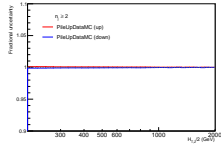
JES Uncertainty in $H_{T,2}/2$ (Single)

Inclusive 2-jet (Top) and Inclusive 3-jet (Bottom)

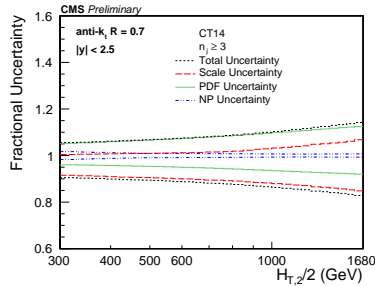
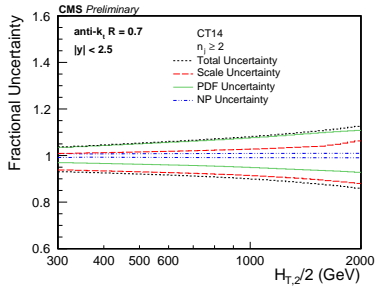


JES Uncertainty in $H_{T,2}/2$ (Single)

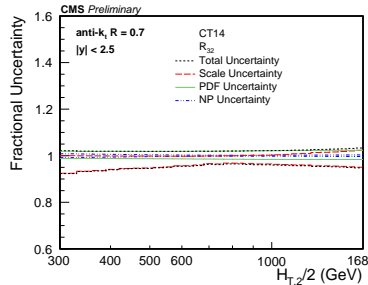
Inclusive 2-jet (Top) and Inclusive 3-jet (Bottom)



Theoretical Uncertainties (CT14)

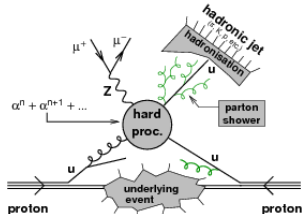


Uncertainty Source	Inclusive 2-jet	Inclusive 3-jet	R ₃₂
Scale	5 to 13%	11 to 17%	6 to 8%
PDF	2 to 10%	5 to 11%	2 to 3%
NP	4 to 5%	4 to 5%	1%



Jets :

- key component to extend our understanding of the Standard Model physics
- signatures of large momentum transfers at short distances, belong primarily to perturbative domain of Quantum Chromodynamics (pQCD)
- produced abundantly in the collisions of protons at the Large Hadron Collider (LHC)
- important backgrounds for many new physics models



Inclusive jet cross section measurement :

- gives important information about the strong coupling constant α_S

$$\sigma_{i\text{-jet}} = \sigma(pp \rightarrow i \text{ jets} + X) \propto \alpha_S^i$$

- provides a deep insight to understand the proton structure by deriving constraints on the parton distribution functions (PDFs)

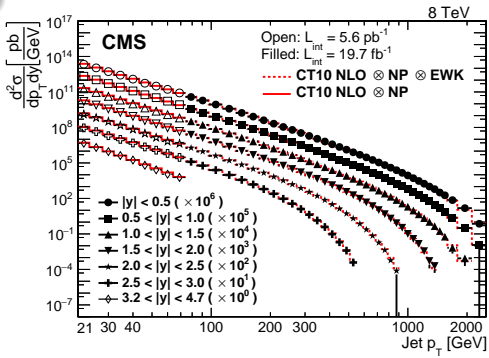
$$\begin{aligned} \sigma_{P_1 P_2 \rightarrow X} &= \sum_{i,j} \int dx_1 dx_2 f_{i,P_1}(x_1, \mu_f) f_{j,P_2}(x_2, \mu_f) \\ &\times \hat{\sigma}_{ij \rightarrow X} \left(x_1 p_1, x_2 p_2, \alpha(\mu_r^2), \frac{Q^2}{\mu_f^2} \right) \end{aligned}$$

Inclusive jet production @ 8 TeV

Double-differential cross-section

$$\frac{d^2\sigma}{dp_T dy} = \frac{1}{\epsilon \mathcal{L}_{int,eff}} \frac{N_{jets}}{\Delta p_T (2\Delta|y|)}$$

- Measurement at 8 TeV
 $\mathcal{L} = 19.7 \text{ fb}^{-1}$ and $\mathcal{L} = 5.6 \text{ pb}^{-1}$
- anti- k_t jets with $R = 0.7$
- $21 \leq p_T < 74 \text{ GeV}$, upto $|y| = 4.7$
- $74 \leq p_T < 2500 \text{ GeV}$, upto $|y| = 3.0$
- Theoretical NLO calculations :
 - using CT10 PDF set
 - corrected for non-perturbative (NP) and electroweak (EWK) effects



JHEP 03 (2017) 156

Inclusive jet production @ 8 TeV

Data/theory using the CT10 NLO PDF :

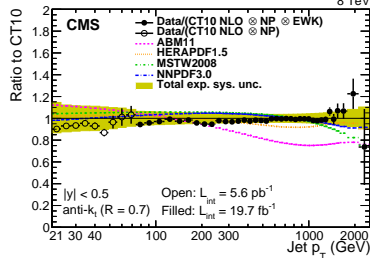
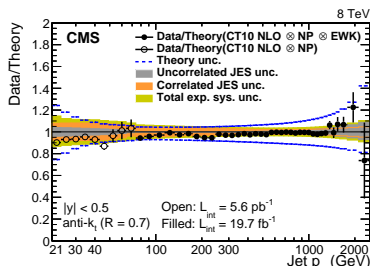
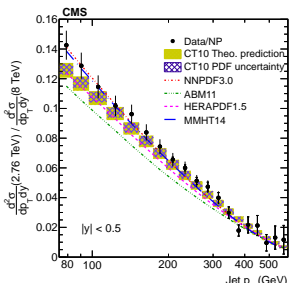
- Good agreement except low-region
- Data uncertainties : jet energy scale (1-45%), lumi (2.6%)
- NLO uncertainties : scale (5-40%), PDF (10-100%)

Ratios to CT10 PDF :

- Significant discrepancies with ABM11 PDF

Ratios 2.76/8 TeV, 7/8 TeV :

- Partial reduction of uncertainties → better sensitivity to PDFs



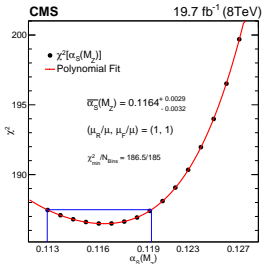
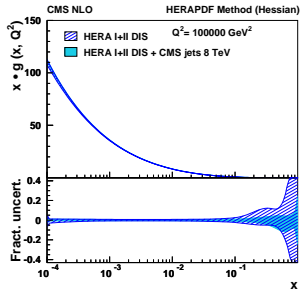
JHEP 03 (2017) 156

QCD analysis using HeraFitter (1.1.1)

- Inclusive cross sections + HERA inclusive DIS :
 - probes hadronic parton-parton interaction over a wide range of x and Q
 - constraints on PDFs
 - significant improvement of the gluon distribution

Extraction of α_S

- Least square minimization on $p_T(y)$ spectrum :
 - using the CT10 NLO PDF set
 $\alpha_S(M_Z) = 0.1164^{+0.0060}_{-0.0043}$
 - using the NNPDF3.0 NLO PDF set
 $\alpha_S(M_Z) = 0.1172^{+0.0083}_{-0.0075}$
- Consistent with the world average value :
 $\alpha_S(M_Z) = 0.1181 \pm 0.0011$



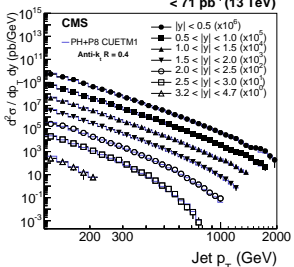
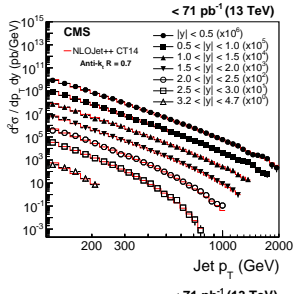
JHEP 03 (2017) 156

Inclusive jet production @ 13 TeV

Double-differential cross-section

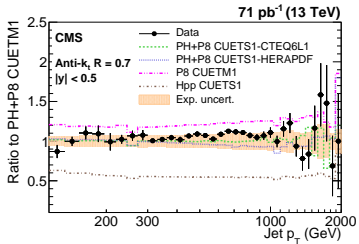
$$\frac{d^2\sigma}{dp_T dy} = \frac{1}{\epsilon \mathcal{L}_{int,eff}} \frac{N_j}{\Delta p_T \Delta y}$$

- Measurement at 13 TeV
 $\mathcal{L} = 71 \text{ pb}^{-1}$ and $\mathcal{L} = 44 \text{ pb}^{-1}$
- anti- k_t jets with $R = 0.4$ and $R = 0.7$
- $< 2 \text{ TeV}$
- Large rapidity coverage : $|y| < 3$, $3.2 < |y| < 4.7$
- Theoretical NLO calculations :
 - using CT14 PDF set
 - corrected for non-perturbative (NP) and electroweak (EWK) effects
- x-sections accurately described for $R = 0.7$, while for $R = 0.4$ theory overestimates by 5–10%

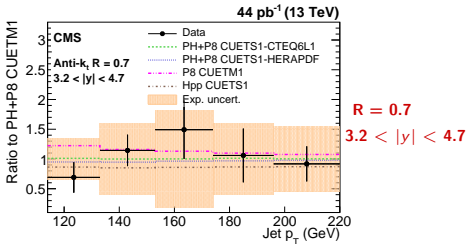


Inclusive jet production @ 13 TeV

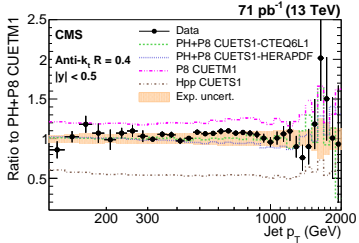
R = 0.7
 $|y| < 0.5$



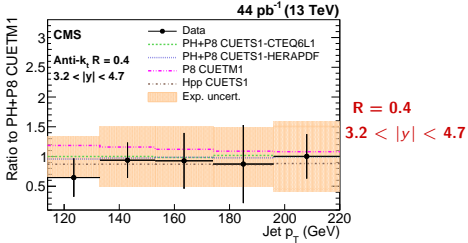
R = 0.7
 $3.2 < |y| < 4.7$



R = 0.4
 $|y| < 0.5$

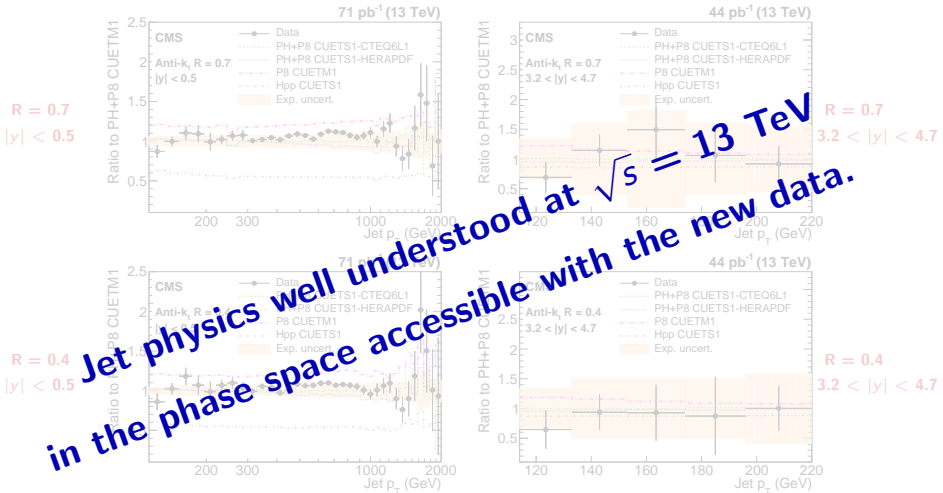


R = 0.4
 $3.2 < |y| < 4.7$



- PYTHIA8 CUETM1 (LO) agrees well in shape for only $|y| < 1.5$.
- HERWIG++ CUETS1 (LO) agrees in shape for all rapidity bins.
- POWHEG+PYTHIA8 (NLO) with various tunes show good agreement for both R.

Inclusive jet production @ 13 TeV



- PYTHIA8 CUETM1 (LO) agrees well in shape for only $|y| < 1.5$.
- HERWIG++ CUETS1 (LO) agrees in shape for all rapidity bins.
- POWHEG+PYTHIA8 (NLO) with various tunes show good agreement for both R.

Triple-Differential dijets

Triple differential cross-section

$$\frac{d^3\sigma}{dp_{T,\text{avg}} dy^* dy_b} = \frac{1}{\epsilon \mathcal{L}_{\text{int}}^{\text{eff}}} \frac{N}{\Delta p_{T,\text{avg}} \Delta y^* \Delta y_b}$$

- Measurement at 8 TeV, $\mathcal{L} = 19.7 \text{ fb}^{-1}$
- anti- k_t jets with $R = 0.7$

Cross section as a function of the :

- ▶ average transverse momentum,

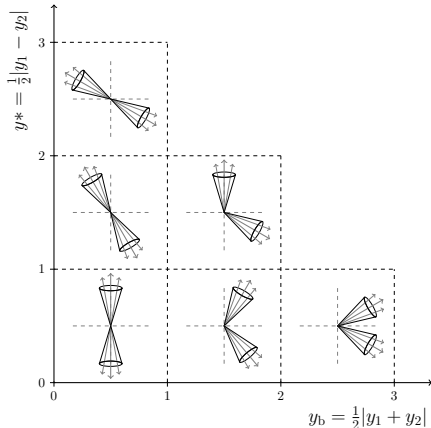
$$p_{T,\text{avg}} = \frac{1}{2}(p_{T,1} + p_{T,2})$$

- ▶ half the rapidity separation,

$$y^* = \frac{1}{2}|y_1 - y_2|$$

- ▶ boost of the two leading jets,

$$y_b = \frac{1}{2}|y_1 + y_2|$$



EPJC 77 (2017) 746

Triple-Differential dijets

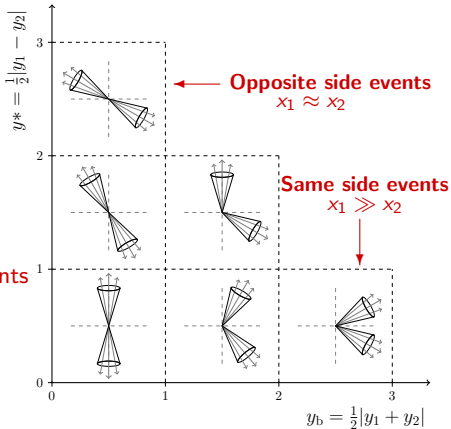
Triple differential cross-section

$$\frac{d^3\sigma}{dp_{T,\text{avg}} dy^* dy_b} = \frac{1}{\epsilon \mathcal{L}_{\text{int}}^{\text{eff}}} \frac{N}{\Delta p_{T,\text{avg}} \Delta y^* \Delta y_b}$$

- Dijet rapidities and the parton momentum fractions are related :

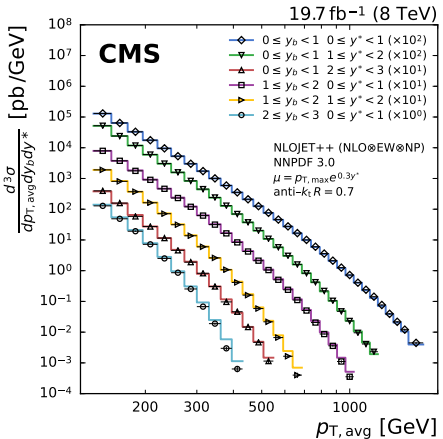
$$x_{1,2} = \frac{p_T}{\sqrt{s}} (e^{\pm y_1} + e^{\pm y_2})$$

- For small y_b , $x_1 \approx x_2 \rightarrow \text{Opposite side events}$
- For large y_b , $x_1 \gg x_2 \rightarrow \text{Same side events}$
(Boosted region)



Triple-Differential dijets

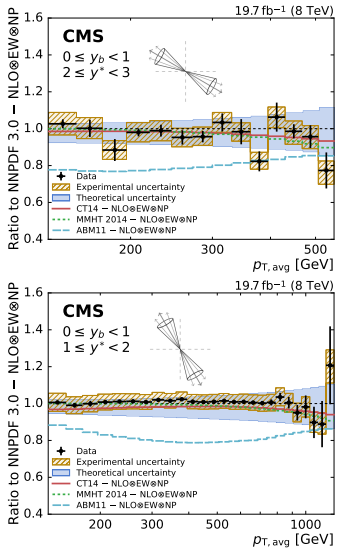
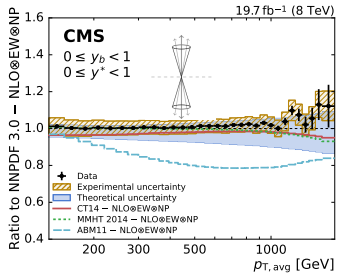
- $p_{T,\text{avg}}$ spectrum for six phase-space regions in y^* and y_b
- Theoretical NLO predictions :
 - ▶ using NLOJET++ with NNPDF 3.0 PDF set
 - ▶ corrected for non-perturbative (NP) and electroweak (EW) effects
- Data are well described by NLO predictions except for the boosted region.



EPJC 77 (2017) 746

Triple-Differential dijets

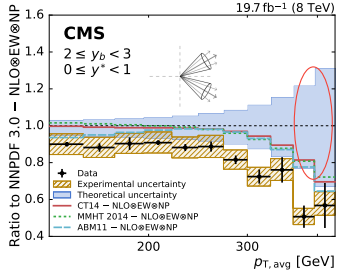
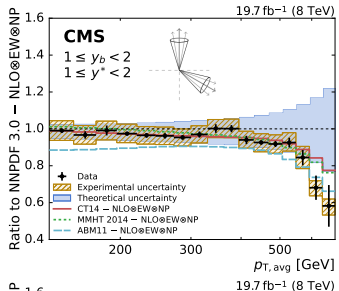
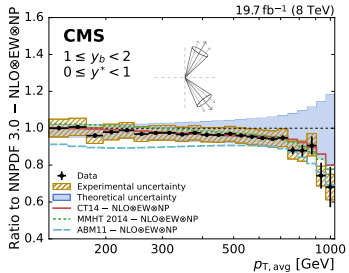
- Ratios to NNPDF 3.0 - NLO \otimes EW \otimes NP
- Data points with statistical uncertainty
- Experimental uncertainty
- Theoretical uncertainty (PDF, Scale and NP)
- Good agreement with MMHT2014 and CT14 PDF NLO calculations
- ABM11 PDF underestimates the predictions



EPJC 77 (2017) 746

Triple-Differential dijets

- Data are well described in most of the analysed phase spaces.
- Differences observed at high $p_{T,\text{avg}}$ and y_b : less known high x region of the PDFs is probed.
- Smaller data uncertainties : potential to constrain the PDFs.



EPJC 77 (2017) 746

Triple-Differential dijets

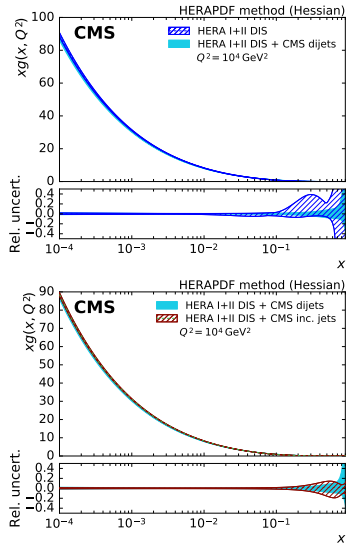
QCD analysis using XFitter (1.2.2)

- Dijet cross sections + HERA inclusive DIS :
 - ▶ an increased gluon PDF at high x with reduced uncertainties of the PDFs
 - ▶ change in shape especially at low Q^2
- Comparison of gluon PDFs with inclusive jet data :
 - ▶ similar shapes of the PDFs and the uncertainties
- Precise α_S extraction together with PDF fit :

$$\alpha_S(M_Z) = 0.1199 \pm 0.0015 \text{ (exp)} \quad {}^{+0.0031}_{-0.0020} \text{ (theo)}$$

- Agreement with the world average value :

$$\alpha_S(M_Z) = 0.1181 \pm 0.0011$$



EPJC 77 (2017) 746

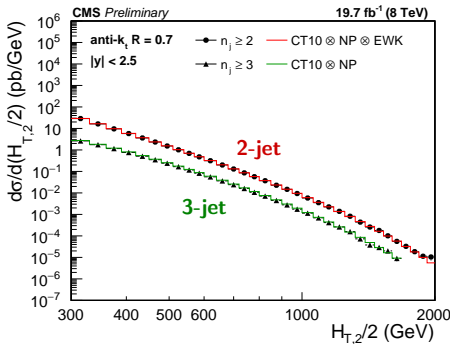
Differential cross-section

$$\frac{d\sigma}{d(H_{T,2}/2)} = \frac{1}{\epsilon \mathcal{L}_{int,eff}} \frac{N_{event}}{\Delta(H_{T,2}/2)}$$

- Measurement at 8 TeV, $\mathcal{L} = 19.7 \text{ fb}^{-1}$
- anti- k_t jets with $R = 0.7$
- 2-jet and 3-jet event cross sections as a function of :**

$$H_{T,2}/2 = \frac{1}{2}(p_{T,1} + p_{T,2})$$

- Theoretical NLO calculations :
 - using CT10 PDF set
 - corrected for non-perturbative (NP) and electroweak (EWK) effects



CMS-PAS-SMP-16-008

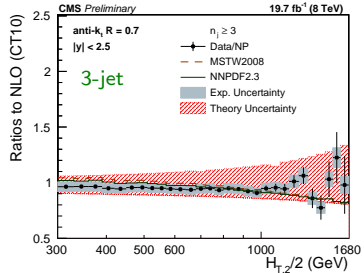
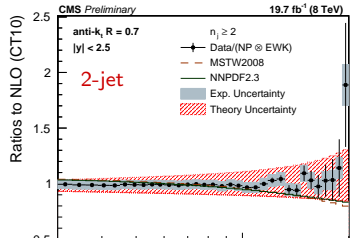
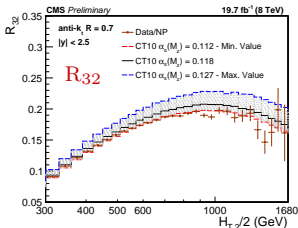
Inclusive multijets

Multijet cross sections

- Data are well described by theory predictions within uncertainty.
- EWK corrections explain the increasing excess of the 2-jet data w.r.t. theory (~ 1 TeV).

Cross section ratio

- $R_{32} = \frac{\sigma_{3\text{-jet}}}{\sigma_{2\text{-jet}}} \sim \alpha_S$
- Experimental uncertainties, theory uncertainties due to NP effects, PDFs, scale choice, EWK corrections may cancel partially or fully
- Better tool to extract α_S

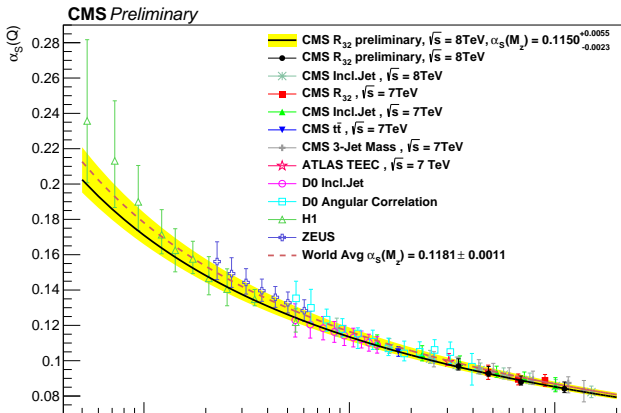


CMS-PAS-SMP-16-008

Inclusive multijets

Determination of α_s

- By minimizing the χ^2 between the measurement and the theory
- In a fit to R_{32} , using the MSTW2008 PDF set :
 $\alpha_s(M_Z) = 0.1150 \pm 0.0023(\text{all except scale})^{+0.0050}_{-0.0000}(\text{scale})$
- $\alpha_s(M_Z)$ extracted in ranges of $H_{T,2}/2 \rightarrow$ evolved to $\alpha_s(Q)$

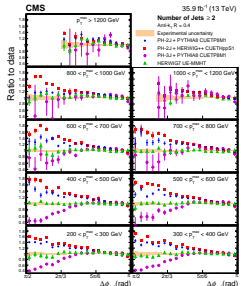
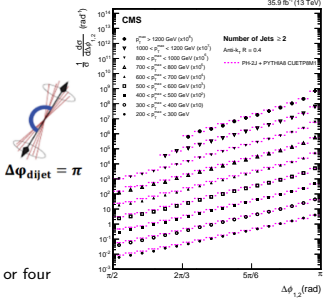


Azimuthal correlations

Normalized differential cross-section

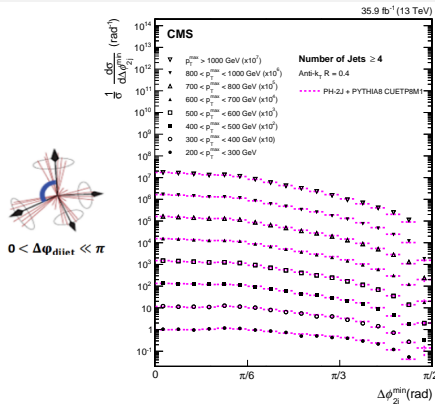
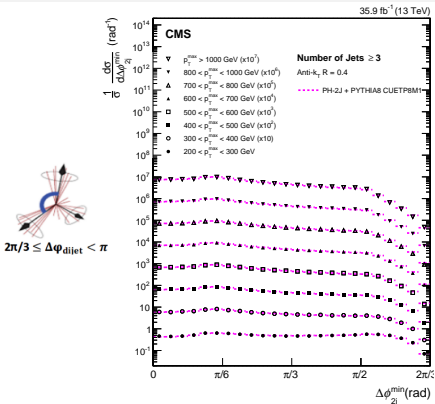
$$\frac{1}{\sigma} \frac{d\sigma}{d\Delta\phi_{1,2}}, \quad \frac{1}{\sigma} \frac{d\sigma}{d\Delta\phi_{2j}^{\min}} \text{ (3-jet and 4-jet)}$$

- Measurement at 13 TeV, $\mathcal{L} = 35.9 \text{ fb}^{-1}$
- anti- k_t jets with $R = 0.4$
- Normalized cross sections as a function of the :
 - azimuthal angular separation between the two highest leading jets
 - minimum azimuthal angular separation between any two of the three or four leading jets (3-jet and 4-jet)
- Spectrum gets flatter and become more sensitive to parton shower on moving from 2-jet to 3-jet to 4-jet
- Best agreement is given by Herwig7
- POWHEG-2J gives better results when matched with Pythia8 than Herwig++
- POWHEG-3J+Pythia8 is generally lower than POWHEG-2J+Pythia8



arXiv:1712.05471 (Submitted to EPJC)

Azimuthal correlations



- Pythia8 (LO) exhibits small deviations from the $\Delta\phi_{1,2}$ and fails to describe $\Delta\phi_{2j}^{min}$
- Herwig++ exhibits the largest deviations from the $\Delta\phi_{1,2}$ but provides a reasonable description of the $\Delta\phi_{2j}^{min}$
- MADGRAPH+Pythia8 provides a good overall description of the measurements except for $\Delta\phi_{2j}^{min}$ in 4-jet case
- An interesting tool to test the theoretical predictions of multijet production processes

Summary

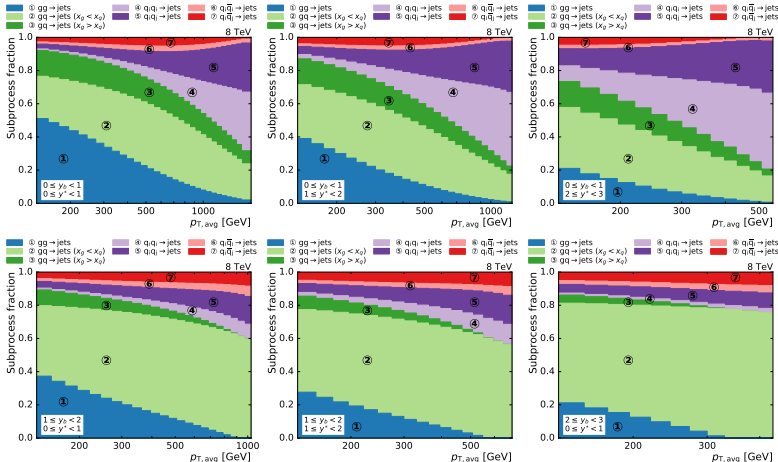
- Jet production in pp collisions is one of the main phenomenological predictions of pQCD.
- Many interesting results from CMS^{*}, reaching new levels of precision and exploring new regions of phase space :
 - ▶ Measurements of differential jet cross sections over a wide range in transverse momenta from inclusive jets to multi-jet final states are presented.
 - ▶ Compared to theoretical predictions including those matched to parton shower and hadronization.
 - ▶ Impact on the determination of the strong coupling constant α_S as well as on parton density functions (PDFs) are reported.
- Wide range of jet measurements at various collision energies improve our understanding of QCD.

THANKS!!

* <http://cms-results.web.cern.ch/cms-results/public-results/publications/SMP/index.html>

Back-Up Slides

Triple-differential dijets



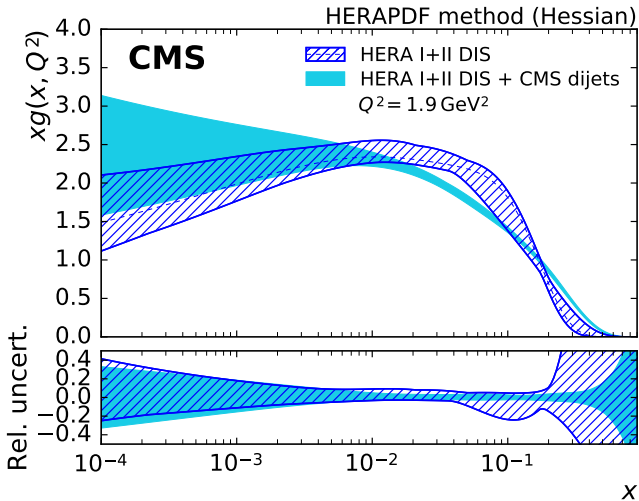
EPJC 77 (2017) 746

Triple-differential dijets

Data set	n_{data}	HERA data		HERA & CMS data	
		χ^2_{P}	$\chi^2_{\text{P}}/n_{\text{data}}$	χ^2_{P}	$\chi^2_{\text{P}}/n_{\text{data}}$
NC HERA-I+II $e^+ p$ $E_p = 920 \text{ GeV}$	332	382.44	1.15	406.45	1.22
NC HERA-I+II $e^+ p$ $E_p = 820 \text{ GeV}$	63	60.62	0.96	61.01	0.97
NC HERA-I+II $e^+ p$ $E_p = 575 \text{ GeV}$	234	196.40	0.84	197.56	0.84
NC HERA-I+II $e^+ p$ $E_p = 460 \text{ GeV}$	187	204.42	1.09	205.50	1.10
NC HERA-I+II $e^- p$	159	217.27	1.37	219.17	1.38
CC HERA-I+II $e^+ p$	39	43.26	1.11	42.29	1.08
CC HERA-I+II $e^- p$	42	49.11	1.17	55.35	1.32
CMS triple-differential dijet	122	—	—	111.13	0.91
Data set(s)		n_{dof}	χ^2	χ^2/n_{dof}	χ^2
HERA data		1040	1211.00	1.16	—
HERA & CMS data		1162	—	—	1372.52
					1.18

EPJC 77 (2017) 746

Triple-differential dijets



EPJC 77 (2017) 746